R. & M. No. 3533

MINISTRY OF TECHNOLOGY

AERONAUTICAL RESEARCH COUNCIL

REPORTS AND MEMORANDA

Two-dimensional Laminar Compressible Boundary-layer Programme for a Perfect Gas

By C. C. L. Sells

LONDON: HER MAJESTY'S STATIONERY OFFICE

1968

PRICE £1 2*s*. 6*d*. NET

Two-dimensional Laminar Compressible Boundary-layer Programme for a Perfect Gas

By C. C. L. Sells

Reports and Memoranda No. 3533*
August, 1966

Summary.

A computer programme has been written to solve the steady laminar two-dimensional boundary-layer equations for a perfect gas at given wall temperature, without wall suction. The programme solves the equations at a blunt stagnation point and then solves the equations downstream. Versions for Mercury and Atlas are available. The Atlas programme will permit use of linear or Sutherland viscosity laws. In an Appendix directions are given for setting up problems for solution; the inviscid edge velocity and wall enthalpy, as functions of downstream arclength along the body, are at the programmer's disposal. It appears possible to obtain results correct to at least three significant figures, usually more not too near separation.

LIST OF CONTENTS

*Replaces R.A.E. Tech. Report No. 66 243—A.R.C. 28 503.

LIST OF APPENDICES

LIST OF TABLES

1. *Introduction.*

It has long been known that incompressible boundary-layer theory is inadequate to deal with many viscous flow and heat-transfer problems involving high-speed aircraft. Accordingly, the compressible boundary layer has been the object of intensive study, beginning with Prandtl[1].

Some specialisation has been almost unavoidable. Mathematically, even in the two-dimensional case one faces the tremendous task of solving two coupled non-linear partial differential equations, and some simplification of the basic problem is needed before a purely analytical solution may be attempted. The layer with zero pressure gradient (flat plate) has been studied by Kármán[2] and Chapman and Rubesin[3], who consider an arbitrary surface-temperature distribution. The case of zero heat transfer at the wall has been considered by Howarth[4] and Stewartson[5], who introduce transformations to reduce the momentum equation to its incompressible form. Similar solutions are found by Cohen and Reshotko[6] and are tabulated for many values of pressure-gradient parameter and wall enthalpy. Other similar solutions for fluids with variable properties, and injection at the wall, have been found by Gross and Dewey[7], who present their results in graphical form. A general discussion of results is available[8].

In many cases, including some of those mentioned above, the assumption of unit Prandtl number and linear viscosity-temperature variation simplifies the equations; Young[9] employs a generalised Pohlhausen method to study the effect of perturbations of Prandtl number and viscosity-temperature index ω from unity (a possible law is: viscosity proportional to ω-th power of temperature). Matting[10] has solved the equations for axisymmetric flow by an expansion in powers of enthalpy difference between the wall and the free stream, with universal functions (including a set of constants depending on the fluid) as coefficients, the expansion being valid near the stagnation point. It is appropriate to remark here that Mangler[11] has shown how to relate any axisymmetric boundary-layer problem to a corresponding two-dimensional one.

This Report describes a computer programme to solve the equations in which no simplifications are made beyond two-dimensional steady flow of a perfect gas in equilibrium. The Prandtl number is assumed to be constant but not necessarily unity. This programme uses a finite-difference method for the values at points of a mesh of transverse and downstream lines, and 'marches' downstream from an initial profile at the stagnation point, utilising the parabolic nature of the equations. The method differs from that of Smith and Clutter[12], who divide the downstream range into intervals but integrate numerically across the layer, using trial values of skin friction and heat transfer and iterating on these until the outer boundary conditions are satisfied. Flügge-Lotz and Blottner[13] also use a mesh method, but they are satisfied with a single guess and trial calculation for the non-linear difference equations, and their solutions will not be particularly accurate, unless the mesh size is very small. They also work with physical variables instead of transforms, which introduces difficulties such as the need to add a certain number of transverse mesh points at downstream stages to allow for boundary-layer growth.

Near separation the programme fails, and other methods will be needed to march past this point (*see* Catherall and Mangler[14] for an example of success in this field). Stewartson[15] has shown that almost certainly a general laminar compressible boundary layer can develop a singularity at the separation point only if the heat transfer there is zero; it was not possible to tell whether this was the case in a trial run, as truncation errors due to finite mesh size were appearing in the results. As a reversed-flow zone appears after separation, so that in some measure the solution depends on downstream conditions as well as upstream, breakdown is not surprising. Moreover, any solutions constructed in some manner from upstream conditions alone will necessarily contain an element of indeterminacy.

2. *The Boundary-layer Equations.*

Consider the steady, two-dimensional flow of a perfect gas in equilibrium past a non-porous rigid body. Let x be the dimensionless distance measured along the body from some fixed point, for example the stagnation point in the case of a blunt body, and y^* dimensionless distance measured normal to body surface at the point given by x. These distances are scaled with respect to some characteristic length l of the system. Further, let u and v^* be dimensionless velocities in the x, y^* directions which have been scaled with respect to the free stream velocity U_∞; let ρ and μ be similarly scaled density and viscosity, and finally scale the pressure p and enthalpy h by factors $\rho_\infty U_\infty^2$ and U_∞^2 respectively. The suffix ∞ refers to free stream values.

The Navier-Stokes equations written in these variables involve the Reynolds number $R = \rho_\infty l U_\infty/\mu_\infty$. Solutions are sought, valid in the limit of infinite Reynolds number, and good for large values also. If we further write

$$y^* = R^{-\frac{1}{2}} y, \qquad v^* = R^{-\frac{1}{2}} v \tag{1}$$

and ignore terms $0(R^{-\frac{1}{2}}, R^{-1}, \ldots)$, the familiar boundary-layer equations are found: (σ is Prandtl number in equation (5))

$$\frac{\partial}{\partial x}(\rho u)+\frac{\partial}{\partial y}(\rho v) = 0 \tag{2}$$

$$\rho u\frac{\partial u}{\partial x}+\rho v\frac{\partial u}{\partial y}=-\frac{\partial p}{\partial x}+\frac{\partial}{\partial y}\left(\mu\frac{\partial u}{\partial y}\right) \tag{3}$$

$$0=\frac{\partial p}{\partial y} \tag{4}$$

$$\rho u\frac{\partial h}{\partial x}+\rho v\frac{\partial h}{\partial y}=u\frac{\partial p}{\partial x}+\mu\left(\frac{\partial u}{\partial y}\right)^2+\frac{\partial}{\partial y}\left(\frac{\mu}{\sigma}\frac{\partial h}{\partial y}\right). \tag{5}$$

These are, respectively, the equation of continuity, the equations of momentum in x and y directions and the energy equation. In addition we require the equation of state

$$h=\frac{\gamma}{\gamma-1}\frac{p}{\rho} \tag{6}$$

and the viscosity as a function of the thermodynamic variables. We shall work with two possible viscosity laws, both of the form

$$\mu=\mu(h) \tag{7}$$

one of which is Sutherland's formula

$$\mu=\left(\frac{h}{h_\infty}\right)^{3/2}\left(\frac{h_\infty+S_u}{h+S_u}\right) \tag{8}$$

where

$$S_u=\left(\frac{C_p}{U_\infty^2}\right)(114°K) \tag{9}$$

C_p being the specific heat at constant pressure, in suitable units so that the Sutherland constant S_u is dimensionless and the same in all unit systems. (U_∞^2 comes in because h and h_∞ have been scaled by this factor.)

Outside the boundary layer, where viscosity has little effect, Euler's equations hold, and also an inviscid energy equation. These lead to Bernoulli's equation which, in our scaled variables, becomes

$$h+\tfrac{1}{2}q^2=\text{const.}=h_\infty+\tfrac{1}{2}=H_s \tag{10}$$

where $q^2=u^2+v^{*2}$ ($=1$ at a great distance) and H_s is the stagnation enthalpy. We can write h_∞ in terms of the Mach number M of the system, for if T denotes temperature

$$h_\infty=\frac{C_pT}{U_\infty^2}=\frac{\gamma RT}{(\gamma-1)U_\infty^2}=\frac{1}{(\gamma-1)M^2}. \tag{11}$$

We assume that the inviscid solution is known for the body. Then at the surface $y^*\to 0$, $v^*\to 0$ and $q=u=q_e$, say, where the suffix e will now refer to the outer edge of the boundary layer ($y\to\infty$). Then h_e is also known by (10).

The boundary conditions for the system (2) through (5) are now:

$$\begin{aligned} &\text{At} \qquad u = v = 0, \quad h = h_B(x) \text{ say} \\ &\text{As} \qquad y \to \infty: \quad u \to q_e, \quad h \to h_e \end{aligned} \tag{12}$$

(It can be shown that $(u-q_e)$ and $(h-h_e)$ decay to zero exponentially as $y \to \infty$ at the stagnation point, and this behaviour may be expected elsewhere. Goldstein[16] gives some arguments, both mathematical and physical, on this point.)

From (2), there exists a stream function ψ such that

$$\rho u = \frac{\partial \psi}{\partial y}, \quad \rho v = -\frac{\partial \psi}{\partial x}. \tag{13}$$

We also put

$$S = \frac{h + \frac{1}{2}u^2}{H_s} - 1. \tag{14}$$

The system becomes

$$\left(\frac{\partial \psi}{\partial y}\frac{\partial}{\partial x} - \frac{\partial \psi}{\partial x}\frac{\partial}{\partial y}\right) u = \rho_e q_e \frac{dq_e}{dx} + \frac{\partial}{\partial y}\left(\mu \frac{\partial u}{\partial y}\right) \tag{15}$$

$$\left(\frac{\partial \psi}{\partial y}\frac{\partial}{\partial x} - \frac{\partial \psi}{\partial x}\frac{\partial}{\partial y}\right) S = \frac{\partial}{\partial y}\left[\frac{\mu}{\sigma}\frac{\partial S}{\partial y} + \frac{1}{H_s}\mu\left(1 - \frac{1}{\sigma}\right) u \frac{\partial u}{\partial y}\right] \tag{16}$$

while (4) and (6) give

$$\frac{h}{h_e} = \frac{\rho_e}{\rho} \quad \text{at fixed } x. \tag{17}$$

We now apply the Howarth-Dorodnitsyn transformation with an x-dependent coefficient to stretch the y co-ordinate so that the boundary layer lies approximately within the same interval for all x (familiar technique), while keeping the computation stage in view by choosing a field variable which decays to zero at the edge of the layer, an extension of the method of Smith and Clutter[12]. This means that more significant figures may be retained to give the deviation from the asymptotic form in this outer region. The equations are simplified also by writing (7) as

$$\frac{\mu}{\mu_s} = C\frac{h}{H_s} = C\frac{h_e}{H_s}\frac{\rho_e}{\rho} \text{ (from (17))} \tag{18}$$

Suffixes s refer to free stream stagnation values.
The transformations are

$$\psi = (\mu_s \rho_s x q_e)^{\frac{1}{2}} (\phi + \eta) \tag{19}$$

$$\eta + \Delta(x) = \left(\frac{q_e}{\mu_s \rho_s x}\right)^{\frac{1}{2}} \int_0^y \rho(y')dy' \tag{20}$$

where $\Delta(x)$ is a certain function of x. From (19) and (20), (13) gives

$$u = q_e(\phi_\eta + 1). \tag{21}$$

Subscripts η and x will denote differentiation. Since, from (12), $u \to q_e$ as $\eta \to \infty$, the boundary condition on ϕ is first

$$\varphi_\eta \to 0 \quad \text{as} \quad \eta \to \infty$$

or $\varphi \to \text{func}(x)$. We need the function of x to be zero, as explained above, and this may be achieved if η in (19) is subject to a change of origin dependent on x, given by (20). Thus $\Delta(x)$ is determined (and is part of the problem) by the boundary condition

$$\phi \to 0 \quad \text{as} \quad \eta \to \infty. \tag{22}$$

From (10), (12) and (14), we have also

$$S \to 0 \quad \text{as} \quad \eta \to \infty. \tag{23}$$

At the wall, given from (20) by $\eta = -\Delta(x)$, (12) and (19) lead to

$$\phi_\eta = -1 \tag{24}$$

$$\phi = -\eta = \Delta(x) \tag{25}$$

and

$$S = S_B(x), \text{ say} \tag{26}$$

where

$$S_B(x) = \frac{h_B(x)}{H_s} - 1.$$

Equations (15) and (16) now become

$$\frac{h_e}{H_s}\frac{\rho_e}{\rho_s}\frac{\partial}{\partial\eta}(C\,\phi_{\eta\eta}) = -\tfrac{1}{2}\left(1+\frac{x}{q_e}\frac{dq_e}{dx}\right)(\phi+\eta)\phi_{\eta\eta} + \frac{H_s}{h_e}\frac{x}{q_e}\frac{dq_e}{dx}\left(\phi_\eta^2 + 2\phi_\eta - S\right) + $$

$$+ x[\phi_{x\eta}(\phi_\eta+1) - \phi_x\,\phi_{\eta\eta}] \tag{27}$$

$$\frac{h_e}{H_s}\frac{\rho_e}{\rho_s}\frac{\partial}{\partial\eta}\left\{\frac{C}{\sigma}\frac{\partial}{\partial\eta}\left[S + (\sigma-1)\frac{q_e^2}{2H_s}(\phi_\eta^2+2\phi_\eta)\right]\right\} = -\tfrac{1}{2}\left(1+\frac{x}{q_e}\frac{dq_e}{dx}\right)(\phi+\eta)\,S_\eta +$$

$$+ x[S_x(\phi_\eta+1) - \phi_x\,S_\eta]. \tag{28}$$

C is a function of S and ϕ. For the (frequently assumed) linear viscosity-temperature law, μ is proportional to h, and from (18)

$$C = 1. \tag{29}$$

On the other hand, if Sutherland's law (8) is invoked, with the help of (10), (14) and (21), (18) gives

$$C = \frac{\left[S+1-\frac{q_e^2}{2H_s}(\phi_\eta+1)^2\right]^{\frac{1}{2}} B'}{\left[S+B'-\frac{q_e^2}{2H_s}(\phi_\eta+1)^2\right]} \tag{30}$$

where

$$B' = 1+S_w/H_s\,. \tag{31}$$

Equations (22) through (28) form a non-linear system of equations for ϕ and S with two-point boundary conditions. The range of η ($-\Delta(x)$ to ∞) is also a variable of the problem.

We shall concern ourselves only with the special case of constant Prandtl number σ, and with flow beginning at a stagnation point. Thus wedge flows cannot be treated with the parameters adopted. Adaptation to axisymmetric flow would be possible with suitably modified equations and computer programme – *see* Smith and Clutter[12].

3. *Linearisation of the Equations for Iterative Solution.*

The equations (27) and (28), with (30) if required, contain four parameters which all depend on the distribution of edge velocity $q_e(x)$ when the stagnation enthalpy H_s (or the Mach number, by (10) and (11)) is known. The parameters are:

$$\left.\begin{aligned} E' &= \frac{x}{q_e}\frac{dq_e}{dx} \\ F' &= \frac{h_e}{H_s}\frac{\rho_e}{\rho_s} = \left(\frac{h_e}{H_s}\right)^{\gamma/(\gamma-1)} \quad \text{(from the equation of state)} \\ G' &= \frac{H_s}{h_e}\frac{x}{q_e}\frac{dq_e}{dx} = \frac{H_s}{h_e}E' \\ H' &= \frac{q_e^2}{H_s}. \end{aligned}\right\} \tag{32}$$

We remark that, by (10)

$$\frac{h_e}{H_s} = 1-\tfrac{1}{2}H' \tag{33}$$

while

$$E' = \frac{x}{2H'}\frac{dH'}{dx}. \tag{34}$$

Hence the ratio q_e^2/H_s is also sufficient.

Equations (27) and (28) are both parabolic, (27) in ϕ_η and (28) in S; for example, (28) contains S_x and $S_{\eta\eta}$. Consequently, when an initial profile has been obtained at a given x-station, to act as an initial

condition for the parabolic equations, it is possible to take a series of stations separated by small step-length b, to replace the x-derivatives by central differences and to 'march' downstream from the initial station. This is the technique used by Smith and Clutter[12] and by Catherall and Mangler[14]. For a variety of reasons – one being the two-point boundary conditions – it was decided not to attempt the solution of the resulting ordinary differential equations, using the computer's Runge-Kutta integration sub-routines, as done by Smith and Clutter, but instead to divide the transverse (η) range into small steps and to replace the η derivatives by differences also, as done by Catherall and Mangler. This involves truncating the boundary layer at a point where the field variables (which are decaying, probably exponentially, near the edge) are sufficiently small, $\eta = Y$ say; Y is a constant which experience shows can be taken as 5 or 6.

The heart of the method of solution at each step downstream will now be as follows: in the equation (28) for S, say, replace all x-derivatives by central differences, for instance

$$\frac{\partial S}{\partial x} \to \frac{1}{b}(S_{\text{new station}} - S_{\text{last station}})$$

and other quantities, including differenced η-derivatives, by weighted averages, for example

$$\phi \to \theta\, \phi_{\text{new station}} + (1-\theta)\, \phi_{\text{last station}} \tag{34a}$$

where θ is a constant, the 'weight parameter', which lies between 0 and 1. The reason is that the representation for the x-derivative is most accurate at an interior point of the downstream interval, by the first mean-value theorem, and we are really attempting to solve the equations at some such interval point while using the end-station values as unknowns. Next, suppose that a guess has been made at the values ϕ_N and S_N of ϕ and S at the interval points labelled $1, 2, \ldots, N, \ldots$ of the transverse (η) co-ordinate line which is the new x-station. Replace some of the unknown field quantities by their guessed values so as to leave a system of linear equations in the remaining unknowns S_N; for example, the term $S_x \phi_\eta$ becomes

$$\frac{1}{b}(S_{N;\,\text{new station}}^{\text{unknown}} - S_{N;\,\text{last station}})\left[\theta(\phi_\eta)_{N;\,\text{new station}}^{\text{guess}} + (1-\theta)\,(\phi_\eta)_{N;\,\text{last station}}\right].$$

Since the differential equation (28) is of second order in η, the difference equations obtained from centrally differencing all η-derivatives at the N-th interval point will contain S_N, S_{N+1} and S_{N-1}, so that the linear equations possess a tridiagonal matrix and can be solved without much computer labour (there is no need for full scale matrix inversion), as explained in Appendix A. The resulting values are used as new guesses in the other equation and the cycle continues until the values converge by some criterion to be determined. This is the method used by Flügge-Lotz and Blottner[13], but they are content with the values obtained by one iteration only. Also, they take either a fully explicit scheme ($\theta = 0$) or a fully implicit one ($\theta = 1$).

The equation (28) is almost linear in S, and it is fairly clear what must be done here. However, equation (27), which should be used to solve for ϕ, is non-linear in this variable. There are many ways to linearise this equation, but the method used must not decrease the order of the differential equation, nor may it make application of the boundary conditions impossible; also, the linearised differential equation should have the same character as the asymptotic form of the equation for large η. It would be desirable to use a scheme yielding quadratic convergence, as in the Newtonian successive approximation to the zero of a function; however, this would give a form of (27) containing ϕ and all its derivatives up to $\phi_{\eta\eta\eta}$ in the unknown part, not replaced by iteration values, and the matrix of the system of equations would have five diagonals instead of three. So it is better to replace ϕ by its last guessed value wherever it occurs, giving a second-order equation for ϕ_η with an associated tridiagonal matrix, as before. ϕ can then be found by integration from the outer boundary. This sacrifices quadratic convergence, but the other criteria can be satisfied; it turns out that the right method effectively solves for u in the original

equations (3) and (5), when the corresponding terms are compared; further, just as in (5) the operator $(\rho u\,\partial/\partial x+\rho v\,\partial/\partial y)$ is applied to the unknown h, so in (3) and the new version of (27) it is applied to the unknown u with the operator variables u and v replaced by their values guessed by iteration.

We use bracketed superscripts to denote the number of iterations that have been done to obtain the superscripted variables. Suppose we are performing the pth iteration; then $\phi^{(p-1)}$, $S^{(p-1)}$ are known and (27) is linearised to

$$x\left[(\phi_\eta^{(p-1)}+1)\,G_x^{(p)}-\phi_x^{(p-1)}\,G_\eta^{(p)}\right]+G'\left[(\phi_\eta^{(p-1)}+1)\,G^{(p)}+\phi_\eta^{(p-1)}-S^{(p-1)}\right]-\tfrac{1}{2}(1+E')\,(\phi^{(p-1)}+\eta)\,G_\eta^{(p)}$$

$$=F'\frac{\partial}{\partial\eta}\left[C^{(p-1)}\,G_\eta^{(p)}\right] \tag{35}$$

where

$$G^{(p)}=\phi_\eta^{(p)}. \tag{36}$$

The reader is reminded that G' is a constant given by (32).

$C^{(p-1)}$ is calculated from $\phi^{(p-1)}$ and $S^{(p-1)}$. When $\phi^{(p)}$ has been found from (35) and (36), it is used to determine $S^{(p)}$ from the similarly linearised equation (28):

$$x\left[(\phi_\eta^{(p)}+1)\,S_x^{(p)}-\phi_x^{(p)}\,S_\eta^{(p)}\right]-\tfrac{1}{2}(1+E')\,(\phi^{(p)}+\eta)\,S_\eta^{(p)}$$

$$=\frac{1}{\sigma}F'\frac{\partial}{\partial\eta}\left\{C^{(p')}\left[S_\eta^{(p)}+(\sigma-1)\,H'\,\phi_{\eta\eta}^{(p)}\,(\phi_\eta^{(p)}+1)\right]\right\} \tag{37}$$

$C^{(p')}$ is calculated from $\phi^{(p)}$ and $S^{(p-1)}$. The equation (35) is now solved again using the new values, and the cycle continues until convergence is attained.

The problem of coping with the variable range of η, $-\Delta(x)\leqslant\eta\leqslant Y$, with $\Delta(x)$ an unknown of the problem, is best overcome by a linear transformation

$$\zeta=\frac{\eta+\Delta(x)}{Y+\Delta(x)}=\frac{1}{D(x)}(\eta+D-Y) \tag{38}$$

where

$$D=Y+\Delta,$$

so that

$$0\leqslant\zeta\leqslant 1.$$

We have

$$\frac{\partial}{\partial x}\to\frac{\partial}{\partial x}+\frac{D_x}{D}(1-\zeta)\frac{\partial}{\partial\zeta} \tag{39}$$

$$\frac{\partial}{\partial\eta}\to\frac{1}{D}\,\frac{\partial}{\partial\zeta} \tag{40}$$

It is convenient to scale ϕ also and to write

$$\phi=D\varphi \tag{41}$$

so that

$$\left.\begin{aligned} \phi_\eta &= \varphi_\zeta = G \\ \phi_{\eta\eta} &= \frac{1}{D}\varphi_{\zeta\zeta} \end{aligned}\right\} \tag{42}$$

(35) now becomes, on rearranging:

$$G_\zeta^{(p)}\left[x\left\{\frac{D_x}{D}(1-\zeta-\varphi^{(p-1)})-\varphi_x^{(p-1)}\right\}-\tfrac{1}{2}(1+E')\left(\varphi^{(p-1)}+\frac{Y}{D}-1+\zeta\right)-\frac{F'}{D^2}C_\zeta^{(p-1)}\right]+$$

$$+x(\varphi_\zeta^{(p-1)}+1)G_x^{(p)}+G'\left[(\varphi_\zeta^{(p-1)}+1)G^{(p)}+\varphi_\zeta^{(p-1)}-S^{(p-1)}\right]$$

$$=\frac{F'}{D^2}C^{(p-1)}G_{\zeta\zeta}^{(p)}. \tag{43}$$

Since D must also be brought into the iteration scheme, we understand that D means $D^{(p-1)}$. Equation (37) becomes:

$$S_\zeta^{(p)}\left[x\left\{\frac{D_x}{D}(1-\zeta-\varphi^{(p)})-\varphi_x^{(p)}\right\}-\tfrac{1}{2}(1+E')\left(\varphi^{(p)}+\frac{Y}{D}-1+\zeta\right)-\frac{1}{\sigma}\frac{F'}{D^2}C_\zeta^{(p')}\right]$$

$$+x(\varphi_\zeta^{(p)}+1)S_x^{(p)}+\frac{1}{\sigma}(1-\sigma)H'\frac{F'}{D^2}C_\zeta^{(p')}\varphi_{\zeta\zeta}^{(p)}(\varphi_\zeta^{(p)}+1)$$

$$=\frac{1}{\sigma}\frac{F'}{D^2}C^{(p')}\left[S_{\zeta\zeta}^{(p)}-(1-\sigma)H'\varphi_{\zeta\zeta\zeta}^{(p)}(\varphi_\zeta^{(p)}+1)+(\varphi_{\zeta\zeta}^{(p)})^2\right]. \tag{44}$$

From (24), (38) and (41), the boundary conditions on φ in (43) are:

$$\left.\begin{aligned} \varphi_\zeta = G &= -1 \\ \varphi &= 1-Y/D(x) \end{aligned}\right\} \text{ at } \zeta = 0 \tag{45}$$

and since the rate of decay of φ is exponential,

$$\varphi = 0, \qquad G = 0 \text{ at } \zeta = 1. \tag{46}$$

The boundary conditions on S in (44) are as before:

$$\left.\begin{aligned} S &= S_B(x) \qquad (\zeta = 0) \\ S &= 0 \qquad\quad (\zeta = 1) \end{aligned}\right\} \tag{47}$$

The four boundary conditions in (45) and (46) on a third-order equation imply that $D(x)$ can indeed be calculated as well as φ. In fact, this is made the basis of the convergence criterion. A set of guesses is fed into (44) in difference form, from which new S_N are determined with the help of (47). These S_N and the last set of φ_N and D are fed into (43), and the boundary conditions (45), (46) on G are used to determine new G_N. The other boundary condition of (46) is then used to integrate G inwards by the trapezoidal

rule to obtain φ_N. The second boundary condition of (45) now gives $D^{(p)}$ in terms of the value φ_0 at the wall:

$$D^{(p)} = \frac{Y}{1-\varphi_0}. \tag{48}$$

It is found that comparison of $D^{(p)}$ with the value $D^{(p-1)}$ fed in is a sufficient test of convergence, and that convergence will occur almost everywhere upstream of separation, that is, the iteration scheme is stable.

The details of the difference scheme (due in principle to Crank and Nicolson[17]) and solution of equations (due to Leigh[18]) are given in Appendix A.

At each step downstream, it is useful to have some information printed out by the programme. In earlier versions, tables of η, ϕ, $U = \phi' + 1$ and S were printed at intervals of 0·1 in x; later versions printed the parameters, displacement thickness

$$\delta^* = \int_0^\infty \left(1 - \frac{\rho u}{\rho_e q_e}\right) dy \tag{49}$$

and skin friction (drag per unit length)

$$F_D = \mu_B \left(\frac{\partial u}{\partial y}\right)_B. \tag{50}$$

These expressions are transformed to the working variables, and comments made upon computation processes, in Appendix B.

Obviously the programme can be modified to give profiles if desired.

4. *Reduction of Discretization Error.*

The replacement of derivatives with respect to ζ by differences is an approximation because of the finite transverse mesh size a. We can show that

$$\left(\frac{\partial^2 \varphi}{\partial \zeta^2}\right)_N = \frac{1}{a^2}(\varphi_{N+1} - 2\varphi_N + \varphi_{N-1}) + 0(a^2) + 0(a^4) \tag{51}$$

$$\left(\frac{\partial \varphi}{\partial \zeta}\right)_N = \frac{1}{2a}(\varphi_{N+1} - \varphi_{N-1}) + 0(a^2) + 0(a^4). \tag{52}$$

These errors are carried through the entire iteration and marching processes. Hence the final answers will have errors $0(a^2)$ and $0(a^4)$; even when the successive values of $\Delta_M^{(p)}$ converge to within 10^{-5}, the value converged upon may differ from the true value in the fourth or even third decimal place. The difference is the discretization error. Some error is due also to finite b, caused by x-derivatives and weighted averaging, but it is the error due to a with which we are concerned here.

In order to eliminate the error of order a^2, we use Richardson extrapolation. Two calculations are performed, one with a at its smallest possible value (for the Mercury programme) and one with a exactly twice this value. Thus the number s of steps used for the smallest a must be even; on Mercury this requires $s = 94$, since $s \leqslant 95$ (*see* Appendix A). Let us consider Δ. Denote the value of Δ for transverse step length a by ${}^a\Delta$; ${}^0\Delta$ is then the correct value in the limit $a \to 0$, and we have (writing $\ddot{\Delta}$ for second derivative of Δ with respect to transverse step length)

$$
\left.
\begin{aligned}
{}^{a}\Delta &= {}^{0}\Delta + \frac{a^2}{2!}\ddot{\Delta} + 0(a^4) \\
{}^{2a}\Delta &= {}^{0}\Delta + 4\frac{a^2}{2!}\ddot{\Delta} + 0(a^4)
\end{aligned}
\right\} \tag{53}
$$

Eliminating $a^2\,\ddot{\Delta}$ from (53), we have

$$
{}^{0}\Delta = \tfrac{1}{3}(4\,{}^{a}\Delta - {}^{2a}\Delta) + 0(a^4)\,. \tag{54}
$$

It is now possible to get five decimal places of accuracy for Δ.

Similar methods can be applied for $\varphi_{M,N}$ and $S_{M,N}$. As only the mesh points with even values of N are used for the $2a$ calculation, in order to get the values at odd mesh points an interpolation formula is used based on the ${}^{2a}\varphi_{M,N}$; the formula is accurate to $0(a^4)$. Richardson extrapolation is then performed on all these values and they are used as the values at the last station, when calculating $\varphi_{M+1,N}$, etc. This method has a suspected drawback – it may be responsible for some oscillation which increases as we go downstream, and it might be better to do two completely separate 'runs' with different values of a, and extrapolate afterwards as an isolated routine. However, the method used has the advantage of convenience, as it requires only two sets of information besides the ones basically needed, as discussed in Appendix A, while the other method would require four extra sets. Moreover, on Mercury it is frequently convenient to interrupt a run for resumption later, and half as much data again would have to be extracted for use on resumption in the other method (*see* Appendix C).

The values of Δ^* and ϕ''_B (convenient notation for $(\phi_{\eta\eta})_B$), which are measures of the displacement thickness and skin friction respectively, are calculated as part of the solution for steplength a and for steplength $2a$ separately, and values for (a) stored along with ${}^{a}\Delta$, ${}^{a}\varphi_{M,N}$ and ${}^{a}S_{M,N}$ while the values for $(2a)$ are being computed. The reason for this is that an integration has to be done in computing Δ^* (*see* Appendix B), and this integration is liable itself to involve errors of order a^2 which are best absorbed into the Richardson extrapolation. (The original programme performed the integration on the final extrapolated values, and the results were observed to be definitely poorer.)

As the values of $(\varphi_\zeta)_{M,N} = G_{M,N}$ are correct only to order a^2, within the iteration cycle, the value of $\phi''_B = (\phi_{\zeta\zeta})_{M,0}\,D^{-1}$ calculated from (B12) of Appendix B will have an error of order a, and the formula

$$
{}^{0}\phi''_B = 2^{a}\phi''_B - {}^{2a}\phi''_B + 0(a^3) \tag{55}
$$

had to be used instead of (54) in calculating the values reported in the next Section. After these tests reported there, another formula for ϕ''_B was developed, in the alternative forms (B16) and (B24). As both these are correct to $0(a^2)$, ordinary Richardson extrapolation was again employed.

5. *The Initial Profile and Departure therefrom.*

The program requires an initial profile from which to march, and can quite easily be made to calculate one. The boundary layer always starts at $x = 0$, at which point all the terms with x-derivatives in (27) and (28) disappear, and so also in (43) and (44), so that these equations are ordinary differential equations in η (or ζ) for φ and S, with two-point boundary conditions, and the same iteration process is used to solve them. In the weighted averaging process defined by (34a) reference to quantities at the 'last station' is suppressed by fixing $\theta = 1$; thus the averaging leaves all quantities unchanged but the same program can be used.

All the examples done in the next section are blunt stagnation point flows (blunt flows for short), near which q_e is proportional to x so that:

$$
E' = F' = G' = 1, \quad H' = 0
$$

But the program will also cope with wedge flows, and flat plate flows (Blasius flows), for which $q_e = 1$, $E' = F' = 0$ and the momentum equation is uncoupled from the energy equation.

When an initial profile has been calculated at $x = 0$, some care is needed with the first few steps downstream. At the first step $x = b$ the equations do not depend on b explicitly, but only through the four parameters $E' \ldots H'$; thus for blunt flows when the change in these is of order b^2, the solution at $x = b$ should not vary much with b, and we expect to find for instance $d\Delta^*/dx = 0$ at $x = 0$; but for wedge flows and decelerating flows the change in $E' \ldots H'$ is of order b, and the solution is then found to be rather sensitive to the value of θ. The theoretical optimum value is $\theta = 0{\cdot}5$, but in practice this causes the values of Δ^* and ϕ_B'' at successive values of x to oscillate, even for blunt flows. This can usually be cured by choosing a larger value of θ; the best value to take depends on the problem, but 0·7 is a good average first guess. In some cases adjustment of θ may still fail to produce acceptable answers; the next line of attack is to decrease b. This has worked for a decelerating flow $q_e = 1 - x$, at high Mach number $M \geqslant 2$.

Far downstream, if θ is returned to the 'optimum' 0·5, oscillation usually appears again. This is contrary to normal experience, whereby errors tend to die out downstream; it could well be due to the Richardson extrapolation which attempts to return the solution of the *difference* equations to that of the *differential* equations at each step but thereby unbalances the smooth running of the difference scheme. However, this oscillation does not appear (and indeed, can be severely inhibited) when θ is kept a little higher than 0·5, say 0·56; the program is thus arranged to let θ tend to 0·56 as x increases.

6. *Examples and Comparisons.*

In order to test the programme, three special cases were examined and compared with results obtained elsewhere. These were, the incompressible boundary layer on a parabola (Catherall and Mangler[14]); the similar solutions of Cohen and Reshotko[6,19]; finally, some profiles computed at the stagnation point by a different method, using numerical (Runge-Kutta) integration, in which the linear law and the Sutherland law could be employed as desired.

Finally, these two laws were compared in their effect on displacement thickness and skin-friction parameters at the stagnation point, and a new example was run, of subsonic flow past a suitable cooled cylinder, such that the inviscid velocity distribution round the cylinder is a simple function – the shape of the cylinder is not needed in the calculation, and is not considered.

The programme was modified slightly to allow for an adiabatic wall (zero heat transfer instead of prescribed wall enthalpy), with $\sigma \neq 1$, but the enthalpy profiles grew from zero only very slowly with increasing x, and it is not considered worth while to present the results.

6.1. *Incompressible Solution for the Parabola.*

Inspection of the equations of motion (27), (28) and the viscosity law (18) shows that reduction to the incompressible case is obtained by putting

$$C = 1; \frac{h_e}{H_s} = 1; \sigma = 1; S_B(x) \equiv 0. \tag{56}$$

From (32) and (33) we have

$$H' = 0; F' = 1; G' = E'. \tag{57}$$

In terms of the variables used by Catherall and Mangler[14], writing $q = q_e$:

$$J = \xi^2/q^2, \qquad dx = \xi d\xi/q \tag{58}$$

and for the parabola

$$J = 1 + \xi^2. \tag{59}$$

Eliminating J and ξ from (58) and (59),

$$dx = \frac{dq}{(1-q^2)^2}$$

hence

$$x = \tfrac{1}{4} ln \frac{1+q}{1-q} + \tfrac{1}{2} \frac{q}{1-q^2}. \tag{60}$$

This makes $x \to 0$ as $q \to 0$, and $x \to \infty$ as $q \to 1-$. q is calculated at the required x-station by solving (60) numerically, and then substituted into the formula

$$E' = \frac{x}{q} \frac{dq}{dx} = x(1-q^2)^2/q \ (x > 0). \tag{61}$$

As there is no thermal boundary layer, Y was put equal to 4. At this point in the known solution, ϕ was $5{\cdot}20 \times 10^{-7}$ (with $x = 0$).

Fig. 1 shows the agreement between the methods of calculating $\phi(\eta)$ at the stagnation point $x = 0$; values found by both methods lie on the same smooth curve. As ϕ decays exponentially to zero at the outer edge, $\log_{10} \phi$ was used to demonstrate that the significant figures agree throughout the range; a plot of ϕ would not have shown this so well. (Similar considerations were applied to Figs. 3 to 6 later.)

Comparison of downstream results in detail is complicated and tedious, and it was judged that comparison of a few values of Δ would form a sufficient test. The table below shows the agreement in $\Delta(x)$ up to $x = 0{\cdot}2$. The value Δ_{CM} due to Catherall and Mangler is determined from the series expansion for small x:

$$\Delta_{CM}(x) = 0{\cdot}64790 + (0{\cdot}29190)x^2 - (0{\cdot}21528)x^4 + (0{\cdot}20358)x^6 - \ldots\ldots \tag{62}$$

x	0·0	0·025	0·05	0·075	0·10	0·20
Δ	0·64790	0·64793	0·64867	0·64940	6·65077	0·65922
Δ_{CM}	0·64790	0·64808	0·64863	0·64953	0·65080	0·65925

The agreement at the stagnation point $x = 0$ is good; a small error is introduced at the first downstream step, and this is reduced in the next step but is persistent thereafter. Catherall and Mangler encountered this difficulty also, and discussed its cause, which is that the terms in the difference equations at the first step do not involve h, so that the values found at the first step will be about the same for all h. They developed a Görtler series to leave the stagnation point; this method is not available to us, at least without considerable labour, and in the next sub-section we shall see that the error can be reduced in some cases by a change in θ (the weight parameter; *see* Section 3).

The programme is not suitable for the incompressible case for two reasons: it uses two unnecessary sets of storage locations (enthalpy), and on Mercury it takes about 9 seconds per iteration in solving for 94 points across the boundary layer, whereas the Catherall and Mangler programme requires $7\frac{1}{2}$ seconds (a new programme developed by Catherall[20] as a simplification of the present one requires only 2 seconds per iteration).

6.2. *The Similar Solutions of Cohen and Reshotko.*

The variables used by Cohen and Reshotko[6] are:

$$\left.\begin{aligned} dX &= \frac{a_e}{a_s}\,\frac{p_e}{p_s}\,dx \\ dY &= \frac{a_e}{a_s}\,\frac{\rho}{\rho_s}\,dy \end{aligned}\right\} \tag{63}$$

where a_e, a_s are sound speeds at the boundary-layer edge and at free-stream stagnation respectively; the stream function used is defined by

$$\Psi_y = \frac{\rho u}{\rho_0}, \quad \Psi_x = -\frac{\rho v}{\rho_0} \tag{64}$$

and 'velocities' are defined by

$$U = \Psi_Y, \quad V = -\Psi_X \tag{65}$$

so that

$$U = \frac{a_s}{a_e}u\,. \tag{66}$$

The linear viscosity law is assumed.

The similar solution is sought in the form

$$\Psi = f(\eta^*)\left[\frac{2\mu_s U_e X}{\rho_s(m+1)}\right]^{\frac{1}{2}} \tag{67}$$

where

$$\eta^* = \left(\frac{m+1}{2}\,\frac{\rho_s U_e}{\mu_s X}\right)^{\frac{1}{2}} Y \tag{68}$$

so that

$$\frac{U}{U_e} = \frac{u}{q_e} = f'(\eta^*), \tag{69}$$

and the free stream 'velocity' is taken as

$$U_e = C^* X^m\,. \tag{70}$$

The enthalpy function S is defined the same way, as in (14), and σ is taken to be 1. Then the equations solved by Cohen and Reshotko are:

$$\left.\begin{aligned} f''' + ff'' &= \beta(f'^2 - 1 - S) \\ S'' + fS' &= 0 \end{aligned}\right\} \tag{71}$$

with boundary conditions

$$f(0) = f'(0) = 0\,, \quad S(0) = S_B\ ; \quad \lim_{\eta^* \to \infty} f' = 1\,, \quad \lim_{\eta^* \to \infty} S = 0\,. \tag{72}$$

Here

$$\beta = \frac{2m}{m+1} \tag{73}$$

(The dashes here denote differentiation of f and S with respect to η.) Now, if the free stream flow is adiabatic, for our perfect gas

$$\frac{p_e}{p_s} = \left(\frac{h_e}{H_s}\right)^{\gamma/(\gamma-1)} = H^{\gamma/(\gamma-1)}\ ; \quad \frac{\rho_e}{\rho_s} = H^{1/(\gamma-1)}\ ; \quad \frac{a_e}{a_s} = H^{\frac{1}{2}} \tag{74}$$

if for convenience we define $H = \dfrac{h_e}{H_s}$; then by (63)

$$\frac{dX}{dx} = H^{\frac{3\gamma-1}{2\gamma-2}}. \tag{75}$$

Equations (66), (70) and (74) give

$$q_e = H^{\frac{1}{2}} X^m C^*$$

or, writing $C^* = (2c\,H_s)^{\frac{1}{2}}$

$$\tfrac{1}{2}H' = \frac{q_e^2}{2H_s} = c\,.\,H\,.\,X^{2m}. \tag{76}$$

Moreover, by (10) or (33)

$$H + \tfrac{1}{2}H' = 1$$

and eliminating H' with (76) gives

$$H = \frac{1}{1+cX^{2m}}. \tag{77}$$

The constants γ, c, m are still at our disposal in the similar solution. The value $\gamma = 1{\cdot}4$ for air is particularly convenient, for in (75) it makes $(3\gamma-1)/2(\gamma-1) = 4$; c can be set equal to 1, and in flow from a stagnation point $x = 0$ ($X = 0$) we must have q_e proportional to x, so that by (66), (70), (74), (75) and (77) (which give U proportional to q_e, and X proportional to x, near $x = 0$) $m = 1$. Then equations (75) and (77) give

$$x = \int_0^X (1+X_1^2)^4\, dX_1$$

or

$$\frac{x}{X} = 1+\frac{4}{3}X^2+\frac{6}{5}X^4+\frac{4}{7}X^6+\frac{1}{9}X^8. \tag{78}$$

Given $x > 0$, there is an $X > 0$ which satisfies (78). This X is found by the computer, and is then substituted into (77); then the quantities in (33) are given by

$$\left.\begin{aligned} H' &= 2(1-\mathrm{H}) \\ F' &= H^{3\cdot5} \\ E' &= \frac{x}{X}H^5 \\ G' &= \frac{x}{X}H^4 \end{aligned}\right\} \tag{79}$$

From (20) and (68), with (63) and (74),

$$\frac{\eta^*}{\eta+\Delta(x)} = \left(\frac{m+1}{2}\frac{a_e}{a_0}\frac{x}{X}\right) = H^{\frac{1}{2}}\left(\frac{x}{X}\right)^{\frac{1}{2}} \tag{80}$$

This quantity was also calculated and printed at each step downstream. We see that at the stagnation point there is no difference between $(\eta+\Delta)$ and η^*, but that downstream of stagnation the ratio changes (η^* increases relative to $\eta+\Delta$). It is a constant at a given x station, so that the boundary-layer variable is uniformly stretched; this is helpful in comparing the tables.

Cohen and Reshotko give a table for the case $m = 1$, with $S_B = 1$. This boundary condition was used accordingly; $Y = 5$ seemed to be the best value to take to include most of the thermal and velocity boundary layer, and for the Mercury programme 94 transverse steps were used. The easiest variables to compare were the velocity $u/q_e = f' = \phi_\eta+1$, and the enthalpy function S. For the velocity, Fig. 2 shows that the Cohen and Reshotko points and those obtained by the present method lie on the same curve to within three decimal places; interpolation reveals differences in the fourth place. (For $x = 0{\cdot}2$ the calculated (η^*, f') points again lie on the curve (and nearly coincide with the calculated points for $x = 0$), which agrees with the theoretical similarity.) Current programme variables f' and S are interpolated to $\eta^* = 0(0{\cdot}2)4$ and are displayed, together with the corresponding Cohen and Reshotko values, in Table 1; the results again agree to three decimal places, which is as much as could be expected since Cohen and Reshotko give only four places, and moreover we have reason to believe that their tables are only accurate to three places in any case, as we shall now show.

The value of Δ in terms of η^* and f at $x = 0$ is

$$\Delta = \phi(-\Delta) = -\int_{-\Delta}^{\infty}\phi_\eta d\eta = \int_{-\Delta}^{\infty}\left(1-\frac{u}{q_e}\right)d\eta$$

$$= \int_0^{\infty}(1-f')\,d\eta^* = \lim_{\eta^*\to\infty}(\eta^*-f). \tag{81}$$

From Cohen and Reshotko's tables, $\Delta = 0{\cdot}4254$. On the other hand, the current programme (with Richardson extrapolation) applied for 70 steps, 94 steps, and (later, on an Atlas run) with 150 steps,

gives $\Delta = 0{\cdot}42500$ to five figures; increasing Y to 6 makes no difference in the fifth place, although decreasing it to 4 does make a difference here (too much boundary layer cut off); moreover, as we shall see later, the value of a related parameter does not change downstream to this order, and finally, the accuracy obtained (nearly six decimal places) in the Catherall and Mangler comparison suggests that Δ can be calculated to five places in general, certainly at the stagnation point. It is concluded that the present results are probably more accurate than Cohen and Reshotko's tables.

We turn to the related parameter mentioned above. Return to equation (81) for general x. At $x = 0$, $\eta + \Delta = \eta^*$; downstream, equation (80) is invoked and then

$$\Delta(x) = \int_0^\infty (1 - f') \frac{d\eta}{d\eta^*} d\eta^* = \Delta(0) \left[H^{\frac{1}{2}} \left(\frac{x}{X} \right)^{\frac{1}{2}} \right]^{-1}$$

so that we may define Δ_{CR} by

$$\Delta_{CR} = H^{\frac{1}{2}} \left(\frac{x}{X} \right)^{\frac{1}{2}} \Delta(x) = \Delta(0). \tag{82}$$

Consequently the correct value of $\Delta(x)$ at any x is determined in principle.

A programme was written for Atlas (similar to Mercury, but larger and faster) and provision was made for the value of Δ_{CR} to be calculated from $\Delta(x)$ and the parameter (80) at each step.

The values should have been all equal to $\Delta(0)$, and the difference provided an excellent check on the accuracy. As mentioned earlier, 150 transverse steps were used, and the downstream step length was taken as $b = 0{\cdot}005$, $0{\cdot}01$, or $0{\cdot}02$. The accuracy demanded of the iterations was 10^{-6}.

At first the value of the weight parameter $\theta = 0{\cdot}5$ was used, and in all runs oscillation in Δ_{CR} started at the first step downstream. The oscillation tended to be smallest for $b = 0{\cdot}01$, so that decreasing the step length b was not the best way to get more accuracy. When $b = 0{\cdot}01$, the oscillation was about $\pm 25 \times 10^{-6}$ up to $x = 0{\cdot}2$, and increased steadily thereafter. Attempts were made to relate this oscillation to errors due to finite a and b, with the aid of formulae like the Richardson extrapolation rule, with a general power, but they all failed to give a satisfactory answer, and it was concluded that the oscillation was not only not due to finite steplengths, but was considerably larger than errors due to such steplengths. Two possible causes are, the first step from the stagnation point, which introduces difficulties noted in Sub-section 5.1, and the actual manner in which the Richardson extrapolation is used; in this programme the values from the extrapolation are used as the initial values (at the last station) for the next step, whereas it may be better to keep two runs going together, one for twice the transverse step length a of the other, the calculations being performed completely independently, and Richardson extrapolation being done outside the main programme as an incidental. Catherall[20] has done such a 'parallel run' from stagnation point for incompressible flow past a parabola, and finds no oscillation. However, as remarked in Section 4, the present method has the advantage of convenience.

Moreover, the method can be greatly improved by manipulating the parameter θ. As θ was increased from $0{\cdot}5$ the oscillation at the stagnation point became less, and eventually at the value $\theta = 0{\cdot}75$ it disappeared altogether ($s = 150$, $b = 0{\cdot}01$). Table 2 shows how the value of Δ_{CR} now tends to rise very slightly and then to fall away again; as the run was continued, Δ_{CR} continued to decrease, below its correct values so that monotonic instability set in (not shown). The values of Δ_{CR} found for $\theta = 0{\cdot}5$ are given for comparison.

It now seems plausible that the monotonic instability far downstream is due to discretization errors piling up for $\theta \neq 0{\cdot}5$. (Theoretically the error in the equations through replacing x-derivatives by central differences and other quantities by averages is $0(b^2)$ for $\theta = 0{\cdot}5$ and $0(b)$ for $\theta \neq 0{\cdot}5$). The instability can be checked by gradually returning θ to its theoretical optimum, $0{\cdot}5$; no comparisons have been made

to see how this should be done, but the programme has been written to replace θ by its average with 0·5, *viz*

$$\theta_{L+1} = 0{\cdot}5(\theta_L + 0{\cdot}5) \tag{83}$$

at every station $x = 0{\cdot}1\,L$, where L is an integer.

The optimum value θ_0 to start with is a function of the problem; for $\theta_0 = 0{\cdot}5$ or perhaps 0·55, the similar solution with $S_B = -1$ (instead of $S_B = 1$) yields hardly any oscillation and increasing θ_0 to 0·75 produces monotonic instability immediately; for $S_B = 0$, $\theta_0 = 0{\cdot}6$ is a good value, and for $S_B = 2$, $\theta_0 = 0{\cdot}8$ is near the best. In this particular problem, determination of $\theta_0(S_B)$ is easy because the parameter Δ_{CR} is available as a check; however, in a general problem one should have Δ printed out at each step to six decimal places, using 10^{-6} as a convergence limit, and spotlight oscillation by taking differences. In good cases, even some way downstream fourth differences may be required. θ_0 is then varied suitably until the oscillation is minimised. θ_0 must not be set too high at first, because then monotonic instability will set in at once, and this cannot be detected by differencing. Thus the smallest value of θ_0 which just eliminates oscillation is the one to use.

One last comparison with these similar solutions was made. Cohen and Reshotko[19] give a table of displacement thickness Δ^* against wall enthalpy S_B; the current programme was accordingly fed with these values of S_B; and the results are displayed, along with Cohen and Reshotko values, in Table 3.

The negative displacement thickness for $S_B = -1$ (zero wall enthalpy and temperature) indicate that the relative density near the wall is very high.

On the whole the values of Δ^* differ in the third decimal place, except for the incompressible case; as Δ^* is calculated from Δ and an integral over quantities which differ in the fourth place, this is not surprising. We again have reason to believe that our values are better.

It was noted that the first five points nearly lie on a cubic curve; a least squares fit gave

$$\Delta^* = 0{\cdot}64785 + (0{\cdot}76356)S_B - (0{\cdot}03444)S_B^2 + (0{\cdot}00751)S_B^3\,. \tag{84}$$

From (84) $\Delta^* = 2{\cdot}097$ at $S_B = 2$, which differs by 0·02 from the table value; within the range $|S_B| \leqslant 1$, the cubic curve will be accurate to 4 decimal places. The zero of Δ^* occurs at $S_B = -0{\cdot}8135$.

For the similar solution $S_B = 1$, Cohen and Reshotko give the skin friction $f' = \phi_B'$ as 1·7368, and one Atlas run gave 1·73668, using (B16). (The expression (B12) gave 1·73472, which reveals its inadequacy.) The difference is of the order as that found for Δ and Δ^*.

6.3. *Another Method of Obtaining Stagnation Point Profiles.*

At the stagnation point $x = 0$, the differential equations become ordinary (in fact, the leading terms in a Görtler expansion in powers of x are given by these ordinary differential equations in η). The equations are:

$$[C_0\,\phi_0'']' + (\phi_0 + \eta)\,\phi_0'' - \phi_0'^2 - 2\phi_0' + S_0 = 0 \tag{85}$$

$$[C_0\,S_0']' + \sigma(\phi_0 + \eta)\,S_0' = 0\,. \tag{86}$$

These equations are obtained from (27) and (28) with the stagnation point values $E' = F' = G' = 1$, $H' = 0$. Here $\phi_0 = \phi(0,\eta)$, $S_0 = S(0,\eta)$, and dashes denote differentiation with respect to η. Also $C_0 = C(S_0)$, by (30). The boundary conditions for (85) and (86) are:

$$\phi_0(-\Delta_0) = \Delta_0\,, \quad \phi_0'(-\Delta_0) = -1\,, \quad S_0(-\Delta_0) = S_B\,;$$

$$\phi_0\,,\, S_0 \text{ exponentially small as } \eta \to$$

Now, the most accurate way of ensuring that this last condition holds is to integrate (85) and (86) inwards from a suitably chosen outer value of η, η_0 say. (This can be done, because Mercury has a built-in Runge-Kutta integration subroutine for solving coupled ordinary differential equations of first order.) To do this, initial conditions on ϕ_0, ϕ_0', ϕ_0'', S_0 and S_0' are required at η_0. These are derived from the asymptotic solution of (85) and (86) for large η; as $\eta \to \infty$, $C_0 \to 1$ from (30), or $C_0 \equiv 1$ from (29), and from (85), (86),

$$\phi_0''' + \eta\, \phi_0'' - 2\phi_0' + S_0 \sim 0$$

$$S_0'' + \eta\, S_0'\, \sigma \sim 0$$

so that, introducing constants A and B,

$$\begin{aligned} S_0 &\sim \frac{B}{\sigma\eta}\Sigma_\sigma\, e^{-\frac{1}{2}\sigma\eta^2} \\ S_0' &\sim B\, e^{-\frac{1}{2}\sigma\eta^2} \end{aligned} \tag{87}$$

where

$$\int_\infty^\eta \exp\left(-\tfrac{1}{2}\sigma\eta'^2\right)d\eta' = \frac{\Sigma_\sigma}{\sigma\eta}\, e^{-\frac{1}{2}\sigma\eta^2}$$

from which Σ_σ can be asymptotically expanded:

$$\Sigma_\sigma = -1 + \frac{1}{\sigma\eta^2} - \frac{1\cdot 3}{(\sigma\eta^2)^2} + \frac{1\cdot 3\cdot 5}{(\sigma\eta^2)^3} - \cdots\cdots \tag{88}$$

and

$$\begin{aligned} \phi_0 &\sim \left(\frac{B}{\sigma-1}+A\right)\left[\frac{1}{2}\left(\frac{2}{3}+\frac{1}{3}\eta^2\right)+\frac{1}{2}\left(1+\frac{1}{3}\eta^2\right)\Sigma_1\right] e^{-\frac{1}{2}\eta^2} - \\ &\quad -\frac{B}{\sigma(\sigma-1)}\left[\frac{1}{2}\left(\frac{2}{3}+\frac{1}{3}\sigma\eta^2\right)+\frac{1}{2}\left(1+\frac{1}{3}\sigma\eta^2\right)\Sigma_\sigma\right] e^{-\frac{1}{2}\sigma\eta^2} \\ \phi_0' &\sim \left(\frac{B}{\sigma-1}+A\right)\left(\frac{1}{2}\eta+\frac{1}{2}\,\frac{1+\eta^2}{\eta}\,\Sigma_1\right) e^{-\frac{1}{2}\eta^2} - \frac{B}{\sigma-1}\left(\frac{1}{2}\eta+\frac{1}{2}\,\frac{1+\sigma\eta^2}{\sigma\eta}\,\Sigma_\sigma\right) e^{-\frac{1}{2}\sigma\eta^2} \\ \phi_0'' &\sim \left(\frac{B}{\sigma-1}+A\right)(1+\Sigma_1)\, e^{-\frac{1}{2}\eta^2} - \frac{B}{\sigma-1}(1+\Sigma_\sigma)\, e^{-\frac{1}{2}\sigma\eta^2} \end{aligned} \tag{89}$$

where Σ_1 means $(\Sigma_\sigma)_{\sigma=1}$.

When $\sigma = 1$, the solution for ϕ_0 is replaced by

$$\begin{aligned} \phi_0 = A &\left[\frac{1}{2}\left(\frac{2}{3}+\frac{1}{3}\eta^2\right)+\frac{1}{2}\left(1+\frac{1}{3}\eta^2\right)\Sigma_1\right] e^{-\frac{1}{2}\eta^2} \\ &+\frac{B}{2}\left[\left(\frac{4}{3}+\frac{1}{6}\eta^2\right)+\left(\frac{3}{2}+\frac{1}{6}\eta^2\right)\Sigma_1\right] e^{-\frac{1}{2}\eta^2}. \end{aligned}$$

However, this case was not computed.

The value $\eta_0 = 8$ was considered sufficiently large. Parameters A and B were now at our disposal, and when all these values were inserted into (88) and (89) for use as initial conditions at η_0 the equations (85), (86) were integrated inwards until $\phi'_0 = -1$. An alternator routine to decrease the Runge Kutta step length in the neighbourhood of this point was embodied. The value of S_0 was next compared with S_B, while at $\phi'_0 = -1$, $\eta = -\Delta_0$, and ϕ_0 should be Δ_0; so $(\phi_0 + \eta)$ was compared with 0. Effectively two conditions must thus be satisfied by two unknowns, A and B.

Much trouble was experienced in finding A and B; most 2-point and 3-point interpolation formulae after finding the values of $(S_0 - S_B)$ and $(\phi_0 + \eta)$ corresponding to trial values of A and B which were not near their correct values broke down, refused to converge, ran on into large negative values of η, or caused the machine to handle numbers beyond its capacity (10^{78}). In order to find A and B for a given S_B, it was necessary to start from a known case (Catherall and Mangler[14]), $S_B = 0$, and to increase or decrease A and B very slowly, keeping the condition $\phi_0(-\Delta_0) = \Delta_0$, and determining the corresponding values of S_B; thus $A = A(S_B)$, $B = B(S_B)$. Eventually S_B was large enough to enable a polynomial curve for A and B to be computed by least squares; then the required value of S_B could be fed in, the trial values of A and B were calculated and iterations commenced. The iteration scheme was to vary B and keep A fixed at first, and to iterate on $S - S_B \equiv l$, say. If B_1 gave a value $l = l_1$, and B_2 gave a value l_2, then the next value tried was

$$B_3 = \frac{B_2 l_1 - B_1 l_2}{l_1 - l_2}. \tag{90}$$

This scheme is a linear extrapolation to $l = 0$. When l did converge to zero, or rather to $\pm 10^{-6}$, the values of A and of $k = \phi_0 + \eta$ were noted. If successive values of A and k were (A_1, k_1) and (A_2, k_2), then, analogously to (90), the next value of A would be

$$A_3 = \frac{A_2 k_1 - A_1 k_2}{k_1 - k_2}. \tag{91}$$

This method worked quite well for $0 \geqslant S_B \geqslant -0{\cdot}5$, but after this point the programme again refused to converge and/or produced large numbers. The convergence limit set on k usually had to be relaxed, with consequent decrease in accuracy.

The value $\sigma = 0{\cdot}7$ was assumed, since for $T \geqslant 200$ deg K we have $0{\cdot}68 \leqslant \sigma \leqslant 0{\cdot}74$ (Monaghan[21]) and small changes in σ are not important (Young[9]) although calculations of heat transfer may differ considerably from reality if $\sigma = 1$[7]. Profiles were obtained for $S_B = -0{\cdot}4$, with both linear (equation (29)) and Sutherland laws (equation (30)). When Sutherland's formula was used with a Mach number of 0·5, gas ambient temperature 4 deg. C and $\gamma = 1{\cdot}4$, the value of B' in (31) was found to be 1·391. (The formulae (9) and (31) give also

$$B' = 1 + \frac{114/T}{1 + \frac{1}{2}(\gamma - 1)M^2} \tag{92}$$

where T is in deg K.) Profiles determined by both methods are shown in Figs. 3 and 4 for the linear case, and the difference is noticeable only at the outer edge where the assumed boundary conditions $\phi_0 = S_0 = 0$ force the curves apart. (The values of ϕ_0 and S_0 were plotted on a logarithmic scale.) For ϕ_0, the effect is shown of varying Y from 5 to 6; the values with $Y = 5$ are appreciably worse near the outer edge, as one expects.

The values of Δ, Δ^* and ϕ'' do not compare well after the third decimal place. Table 4 presents results from both methods, the matrix programme value being given first. The inferior formula (B12) was used for the matrix values ϕ'', unfortunately. However, the values of $\Delta - \Delta^* = -\int_{-\Delta}^{\infty} S_0 \, d\eta$ (*see* (B4)), agree to four decimal places.

6.4. *Comparison of Linear Law with Sutherland Law at the Stagnation Point.*

We now turn to some independent results, and begin with an examination of the differences due to a change in the viscosity law.

It is known (Young[9]) that, when the viscosity law is of the form

$$\mu \propto^{l} T^{\omega} \tag{93}$$

the value of ω may affect the skin friction considerably. However, ω changes considerably over the temperature range, and Sutherland's formula gives a much better fit; we now examine the case $\omega = 1$ (linear law) and see how the profiles are changed. The Prandtl number σ is again taken as 0·7.

When $S_B = -0{\cdot}4$, the stream functions and enthalpy functions for each case are as shown in Figs. 5 and 6, and are nearly indistinguishable; the values found for Δ, Δ^* and ϕ''_B are given in the first and last columns of Table 4 already referred to. From these values, we see that the difference between the results for Δ and Δ^* is about 4 per cent and for skin friction ϕ''_B is about 5 per cent. The difference increases when the wall enthalpy function S_B is increased (so that the heat transfer increases also); Table 5 shows the results and percentages based on the linear results when $S_B = -0{\cdot}5$ and when $S_B = +1{\cdot}0$, again with $\sigma = 0{\cdot}7$.

It is concluded anew that the linear law may give results sufficiently accurately for some engineering applications, and so is a worthwhile theoretical simplification.

6.5. *Subsonic Flow Past a Cooled Cylinder.*

In order to see how the programme behaved when the pressure gradient became unfavourable downstream, a sinusoidal distribution of edge velocity was fed in, given by

$$q_e = 2 \sin (x/r) \tag{94}$$

where x is arc distance from the stagnation point. This is the inviscid incompressible flow for a circular cylinder of radius r in a uniform stream of unit velocity; in the compressible case, the shape of the cylinder will not be circular and will depend on the Mach number, but this is immaterial; we require only a convenient function for the programme. The diameter $2r$ was taken 1, so that q_e had a maximum at $x = \pi/4 = 0{\cdot}785$, and we took $M = 0{\cdot}5$, $\gamma = 1{\cdot}4$, $\sigma = 0{\cdot}7$. The cylinder was assumed cooled relative to stagnation conditions, and isothermal, and we took the arbitrary value

$$S_B(x) = -0{\cdot}5\,. \tag{95}$$

This was expected to move the separation point downstream. The incompressible separation point is[23] $x/r = 104{\cdot}45°$, so here $x = 0{\cdot}91$. Separation was expected for some $x > 0{\cdot}91$.

The external flow parameters were calculated from (32). The linear viscosity law was assumed.

At first the programme was run on Mercury with 94 transverse steps, $Y = 5, b = 0{\cdot}01, 10^{-5}$ convergence accuracy, and $\theta = 0{\cdot}5$. The machine eventually reached the point $x = 0{\cdot}92$ in about two hours, and then the iterations failed to converge. Inspection of the displacement thickness Δ^* and skin friction φ''_B at successive stations showed increasing oscillation which became noticeable even on a graph after $x = 0{\cdot}7$, and inspection of the profiles showed bad behaviour of the velocity near the outer edge and of the enthalpy near the body – the value one station out (H_1 on the computer) was oscillating between limits of the order $+3{\cdot}0$ and $-1{\cdot}0$, compared with the boundary value $-0{\cdot}5$. Quite clearly the Crank-Nicolson scheme (with $\theta = 0{\cdot}5$) was producing unacceptable numerical instability. An Atlas run with 150 steps (in hopes of reducing the initial error) was no better; oscillation at the stagnation point was visible from third differences in $\Delta(x)$.

A different value of θ_0 was accordingly tried on the Atlas programme. The value $\theta_0 = 0{\cdot}6$ smoothed out the oscillation considerably at the stagnation point, second differences showing its presence in the sixth place; however, at each station $x = 0{\cdot}1\ L$ the averaging of θ with 0·5 according to (83) seemed to

allow oscillation to increase downstream, although not so drastically as before – but it was again unacceptable around $x = 0{\cdot}9$.

By chance a profile taken from this run at $x = 0{\cdot}7$ was fed in again with θ restored to its former value of 0·6, and this time the oscillation damped out within five downstream steps and did not reappear. So the Crank-Nicolson approximation (83) was abandoned and θ was instead made to tend to the value 0·56 downstream, freedom being retained to choose θ_0 to minimise oscillation at $x = 0$; (83) was thus replaced by

$$\theta_{L+1} = 0{\cdot}5\,\theta_L + 0{\cdot}28\,. \tag{83a}$$

The results with $\theta_0 = 0{\cdot}6$ were very satisfactory, oscillation being absent everywhere except near $x = 0$ (not quite best θ_0). Figs. 7 and 8 show the velocity and enthalpy profiles at $x = 0{\cdot}9$; both are characteristic near-separation profiles, and it will be noticed that near $\eta + \Delta = 0$ both curves are beginning to turn over, a point of inflexion appearing, and the gradients diminishing rapidly. Figs. 9, 10 and 11 show the variation with x of Δ, Δ^* and ϕ''_B respectively. From the ϕ''_B curve, or by extrapolation from the numerical results (not presented), we can predict that ϕ''_B will become zero for some x between 0·92 and 0·93; that is, aft of the incompressible separation point, as predicted, but not greatly so. (We must remember, however, that the two bodies are not the same.) A graph of $(\phi''_B)^2$ against x (Fig. 12) gave a fair straight line near separation and confirmed the prediction of the separation point.

No arrangement was made to march right up to separation by halving the steplength, because of lack of time. A routine has been inserted to do this.

We remark that the total number of iterations needed at each step seemed to be insensitive to the values of b and s, depending only on x and the accuracy demanded, when the solution was smooth. With $V' = 10^{-6}$, near $x = 0$, after fluctuating for a few steps, it would settle down to about 6, increase slowly to about 20 at $x = 0{\cdot}8$ and then more rapidly to about 35 at $x = 0{\cdot}9$.

Simple-minded attempts to march past the separation point have failed, as have most others in the past, on account of the singularity which usually prevails at $\phi''_B = 0$. The incompressible programme of Catherall and Mangler[14] prescribes Δ and finds q_e, or rather $x/q_e\, dq_e/dx$ (our E'); as the four parameters E', F', G' and H' are non-linearly connected, at first attempts were made to prescribe Δ, guess a set of parameters and compare resulting $\Delta^{(p)}$ with Δ, but a more promising line is to solve for E' as in the incompressible case, noting that the values of F', G'/E' and H' change only slowly compared with E' and so setting these quantities from the last calculated value of E'. The matrix scheme is more complicated, with the extra unknown, but the problems associated with it have been solved and a pilot programme written by Catherall[20], which appears to converge well and may be the subject of another Report later.

7. Concluding Remarks.

A programme has been written to solve the laminar steady two-dimensional boundary-layer equations for a perfect gas, beginning at a stagnation point. On the Mercury version, for reasons of space and time, only the linear viscosity law is assumed, but an Atlas programme will allow the Sutherland law to be used also (and, if the programmer desires, some other law could be used instead). For those who wish to use the programme for the solution of their own special problems, Appendix C describes the storage locations used and certain facilities available, and contains directions for setting up these problems.

By judicious adjustment of the weight parameter θ to suit any given problem, it appears possible to obtain results correct to at least three significant figures accuracy, and in many cases, especially near the stagnation point, four or five. The limiting factor is the minimal oscillation, which appears to arise because of the use of Richardson-extrapolated results for initial values in a downstream step; if no Richardson extrapolation were used, and the parameters a, b and θ are chosen so that the scheme is stable (Richtmyer[22]), the solution of the *difference* equations is expected to be smooth – but only if the last set of values found is used as the new set of initial values. The effect of attempting to use the extrapolated values instead, these being better approximations to the solution of the *differential* equations, is to destroy this smoothness. It is hoped to write an alternative programme to avoid this defect and to use instead the 'parallel run' method, for use on Atlas if desired.

As mentioned in Sub-section 6.5, near separation the programme fails. To march past this point, Catherall has written a pilot programme analogous to his incompressible programme[14], and preliminary results obtained seem promising.

It will be noticed that the current programme deals with an impermeable wall with a fixed temperature distribution as boundary condition. The boundary condition on S could be altered easily to a condition on heat transfer, but the inclusion of suction effects would entail a little more modification.

APPENDIX A

The Difference Equations and their Solution

The equations (43) and (44) contain first derivatives in x and up to third derivatives in ζ. These derivatives are replaced by central differences in a rectangular mesh in the (x, ζ) plane; let a be the width of the mesh in the (transverse) ζ direction and b the width downstream (x direction). Use an integer N to denote a transverse mesh point, and let N run from 0 (at $\zeta = 0$) to s (at $\zeta = 1$). Clearly $a = 1/s$. For convenience, we may use M as an integer representing the downstream x-station at which the solution is to be determined, so that the previous station is labelled $(M-1)$. We denote the value of a function, φ say, at the M-th downstream and N-th transverse mesh point by $\varphi_{M,N}$. If the quantity φ is still being determined by iteration, it is represented by $\varphi^{(p)}_{M,N}$ at the p-th cycle, as in the equations (43) and (44). This will not be needed at the $(m-1)^{th}$ station, since the solution is known there (by the marching process).

The central difference formula for x-derivatives

$$\left(\frac{\partial \varphi}{\partial x}\right)_{M,N} = \frac{\varphi_{M,N} - \varphi_{M-1,N}}{b} \tag{A1}$$

is an exact identity at some interior point of the interval (x_{M-1}, x_M) and has an error of order b at an end point and of order b^2 at the mid-point. So in order to obtain better accuracy (and stability also) all other quantities, including differences due to ζ derivatives, are replaced by weighted averages of their values at the $(M-1)^{th}$ and Mth stations, the effect being that the equations are solved at an interior point of the interval (x_{M-1}, x_M). Although the error is theoretically smallest at the mid-point, there are reasons why the weight parameter should be a variable at our disposal in the calculation; a judicious choice of this parameter increases the stability of the march downstream, and a suitable choice enables us to use the same programme to calculate an initial profile at the stagnation point, from which to march. We therefore replace x, for example, by

$$\theta\, x_M + (1-\theta)\, x_{M-1} = x_M - (1-\theta)\, b \tag{A2}$$

where θ is the weight parameter, and calculate H' and the other external flow variables at this mean station. φ_ζ is replaced by

$$\left.\begin{aligned} &[\theta\,\{\varphi^{(p)}_{M,N+1} - \varphi^{(p)}_{M,N+1}\} + (1-\theta)\,\{\varphi_{M-1,N+1} - \varphi_{M-1,N-1}\}]/2a \\ \text{and } \varphi^{(p)}_{\zeta\zeta} \text{ by} \\ &[\theta\,\{\varphi^{(p)}_{M,N+1} - 2\varphi^{(p)}_{M,N} + \varphi^{(p)}_{M,N-1}\} + (1-\theta)\,\{\varphi_{M-1,N+1} - 2\varphi_{M-1,N} + \varphi_{M-1,N-1}\}]/a^2 \end{aligned}\right\} \tag{A3}$$

The error in these expressions is $0(a^2)$.

When these and similar expressions are substituted into the momentum equation (43), the following

difference equation is obtained:

$$\alpha_N G^{(p)}_{M,N+1} + \beta_N G^{(p)}_{M,N} + \gamma_N G^{(p)}_{M,N-1} = \delta_N \quad (1 \leqslant N \leqslant s-1) \tag{A4}$$

where we write

$$\left.\begin{aligned} D_\theta &= \theta D_M^{(p-1)} + (1-\theta) D_{M-1} \\ \frac{F'}{a^2 D_\theta^2} &= H \\ \bar{C}_N &= \theta C^{(p-1)}_{M,N} + (1-\theta) C_{M-1,N} \end{aligned}\right\} \tag{A5}$$

$$\begin{aligned} \Lambda = \frac{x}{b}\left[\frac{D_M^{(p-1)} - D_{M-1}}{D_\theta}\left[1-\zeta-\{\theta\varphi^{(p-1)}_{M,N} + (1-\theta)\varphi_{M-1,N}\}\right] - (\varphi^{(p-1)}_{M,N} - \varphi_{M-1,N})\right] + \\ + \tfrac{1}{2}(1+E')\left[1-\zeta-\{\theta\varphi^{(p-1)}_{M,N} + (1-\theta)\varphi_{M-1,N}\} - \frac{Y}{D_\theta}\right] - \\ - \frac{a}{2} H\left[\theta(C^{(p-1)}_{M,N+1} - C^{(p-1)}_{M,N-1}) + (1-\theta)(C_{M-1,N+1} - C_{M-1,N-1})\right] \end{aligned} \tag{A6}$$

and then

$$\alpha_N = \theta\left(\frac{\Lambda}{2a} - H\bar{C}_N\right) \tag{A7}$$

$$\beta_N = \left(\frac{x}{b} + \theta G'\right)\{\theta G^{(p-1)}_{M,N} + (1-\theta) G_{M-1,N} + 1\} + 2H\bar{C}_N \tag{A8}$$

$$\gamma_N = \theta\left(-\frac{\Lambda}{2a} - H\bar{C}_N\right) \tag{A9}$$

$$\begin{aligned} \delta_N = \left\{\frac{x}{b} - (1-\theta) G'\right\} \{\theta G^{(p-1)}_{M,N} + (1-\theta) G_{M-1,N} + 1\} G_{M-1,N} - \\ - G'\left[\{\theta G^{(p-1)}_{M,N} + (1-\theta) G_{M-1,N}\} - \{\theta S^{(p-1)}_{M,N} + (1-\theta) S_{M-1,N}\}\right] + \\ + H(1-\theta)\bar{C}_N (G_{M-1,N+1} - 2G_{M-1,N} + G_{M-1,N-1}) - \\ - \Lambda(1-\theta)(\varphi_{M-1,N+1} - 2\varphi_{M-1,N} + \varphi_{M-1,N-1})/a^2 . \end{aligned} \tag{A10}$$

When $N = s-1$, there are slight changes due to the end point. By (46), $G^{(p)}_{M,S} = 0$. Also, some care will be needed over the penultimate term in δ_N, which involves what is really $(\varphi_{M-1})_{\zeta\zeta\zeta}$. It is found inconvenient to store $G_{M-1,N}$ as well as $\varphi_{M-1,N}$, in the computer's high speed store, so the term in brackets must be replaced by

$$\frac{1}{2a}[\varphi_{M-1,N+2} - 2\varphi_{M-1,N+1} + 2\varphi_{M-1,N-1} - \varphi_{M-1,N-2}] \tag{A11}$$

which includes a term not in the computed set of variables when $N = s-1$. We remember that

$$G_{M,N} = \frac{1}{2a}(\varphi_{M,N+1} - \varphi_{M,N-1}).$$

Here we use the fact that $\varphi = \varphi_\zeta = 0$ at $\zeta = 1$ to develop the formula

$$\frac{1}{2a}[\varphi_{M-1,S-1} + 2\,\varphi_{M-1,S-2} - \varphi_{M-1,S-3}]$$

for use instead of (A11) in (A10).

When $N = 1$, corresponding changes have to be made. From (45), $G^{(p)}_{M,0} = -1$. Again, (A11) contains a term outside the variable set used, and (by (45)) must be replaced by

$$\frac{1}{2a}[\varphi_{M-1,3} - 2\,\varphi_{M-1,2} - \varphi_{M-1,1} + 2\,\varphi_{M-1,0} - 2a].$$

The energy equation (44) yields the following:

$$\alpha^*_N S^{(p)}_{M,N+1} + \beta^*_N S^{(p)}_{M,N} + \gamma^*_N S^{(p)}_{M,N-1} = \delta^*_N \tag{A12}$$

where equations (A6) to (A9) inclusive hold for the corresponding starred variables and in (A5) a factor σ^{-1} is introduced into the second equation so that it reads:

$$\frac{F'}{\sigma a^2 D^2_\theta} = H. \tag{A13}$$

(All bracketed superscripts are now changed from $(p-1)$ to (p) in these equations.) δ^*_N is given by

$$\begin{aligned}
\delta^*_N = {} & \frac{x}{b}[1 + \theta G^{(p)}_{M,N} + (1-\theta) G_{M-1,N}] S_{M-1,N} - \frac{\Lambda}{2a}(1-\theta)(S_{M-1,N+1} - S_{M-1,N-1}) + \\
& + H(1-\theta)(S_{M-1,N+1} - 2\,S_{M-1,N} + S_{M-1,N-1})\,\bar{C}_N - \\
& - H H'(1-\sigma)\Bigg[\bar{C}_N\Big\{[\theta G^{(p)}_{M,N} + (1-\theta) G_{M-1,N} + 1] \times \\
& \times \Big[\theta(G^{(p)}_{M,N+1} - 2\,G^{(p)}_{M,N} + G^{(p)}_{M,N-1}) + \\
& + \frac{1-\theta}{2a}(\varphi_{M-1,N+2} - 2\,\varphi_{M-1,N+1} + 2\,\varphi_{M-1,N-1} - \varphi_{M-1,N-2})\Big] + \\
& + \Big[\tfrac{1}{2}\theta(G^{(p)}_{M,N+1} - G^{(p)}_{M,N-1}) \\
& + \frac{1-\theta}{a}(\varphi_{M-1,N+1} - 2\,\varphi_{M-1,N} + \varphi_{M-1,N-1})\Big]^2\Big\} \\
& + \tfrac{1}{2}(\bar{C}_{N+1} - \bar{C}_{N-1})[\theta G^{(p)}_{M,N} + (1-\theta) G_{M-1,N} + 1] \times
\end{aligned}$$

$$\left[\times\left[\tfrac{1}{2}\theta\,(G^{(p)}_{M,N+1}-G^{(p)}_{M,N-1})+\right.\right.$$

$$\left.\left.+\frac{1-\theta}{a}(\varphi_{M-1,N+1}-2\,\varphi_{M-1,N}+\varphi_{M-1,N-1})\right]\right] \tag{A14}$$

(A12) is treated like (A4) when $N = 1$ or when $N = s-1$. From the boundary conditions (47) $S_{M,s} = 0$ and $S_{M,0} = S_B(x)$ given, and the term (A11) in (A14) is substituted for according to the value of N.

Equations (A4) and (A12) are both systems of $(s-1)$ linear equations in $(s-1)$ unknowns, and the matrices governing the systems are both tridiagonal, of the form

$$\underline{\underline{A}} = \begin{bmatrix} \beta_{s-1} & \gamma_{s-1} & & & & 0 & \\ \alpha_{s-2} & \beta_{s-2} & \gamma_{s-2} & & & & \\ & \alpha_{s-3} & \beta_{s-3} & \gamma_{s-3} & & & \\ & . & . & . & & & \\ & & . & . & . & & \\ & & & . & . & . & \\ & 0 & & & \alpha_2 & \beta_2 & \gamma_2 \\ & & & & & \alpha_1 & \beta_1 \end{bmatrix} \tag{A15}$$

The matrix $\underline{\underline{A}}$ may be factorised into lower and upper triangular matrices $\underline{\underline{L}}$ and $\underline{\underline{U}}$:

$$\underline{\underline{L}}\,.\,\underline{\underline{U}} = \begin{bmatrix} k_{s-1} & . & & & & & \\ l_{s-2} & k_{s-2} & . & & & 0 & \\ . & l_{s-3} & k_{s-3} & & & & \\ & . & . & . & & & \\ & & . & . & & & \\ & & & . & . & & \\ & & & & . & . & \\ & 0 & & & l_2 & k_2 & \\ & & & & & l_1 & k_1 \end{bmatrix} \begin{bmatrix} 1 & u_{s-1} & & & & & \\ & 1 & u_{s-2} & & & 0 & \\ & & 1 & u_{s-3} & & & \\ & & & . & . & & \\ & & & & . & . & \\ & & & & & . & . \\ & & & & & . & . \\ & & & & & 1 & u_2 \\ & & & & & & 1 \end{bmatrix} \tag{A16}$$

Comparing (A15) and (A16), we have:

$$\left.\begin{aligned} l_N &= \alpha_N \,(1 \leqslant N \leqslant s-2) \\ k_{s-1} &= \beta_{s-1} \\ k_N &= \beta_N - \alpha_N u_{N+1} \,(1 \leqslant N \leqslant s-2) \\ k_N u_N &= \gamma_N \,(2 \leqslant N \leqslant s-1) \end{aligned}\right\} \tag{A17}$$

Now, if $\underline{h}$ represents an unknown vector and $\underline{\delta}$ represents the right side of the equation (A4) or (A12) as a column vector, the equation

$$\underline{\underline{A}}\,\underline{h} = \underline{\delta}$$

may be split into

$$\underline{\underline{L}}\,\underline{y} = \underline{\delta} \tag{A18}$$

$$\underline{\underline{U}}\,\underline{h} = \underline{y} \tag{A19}$$

where $\underline{y}$ is a new column vector $(y_{s-1}, y_{s-2}, \ldots, y_1)'$.

Equation (A18) now gives

$$\left.\begin{aligned} k_{s-1}\, y_{s-1} &= \delta_{s-1} \\ k_N\, y_N + \alpha_N\, y_{N+1} &= \delta_N - h_0\, \gamma_1\, [\delta_{1,N}] \,(1 \leqslant N \leqslant s-2)\,. \end{aligned}\right\} \tag{A20}$$

The term $h_0\, \gamma_1\, \delta_{1,N}$ takes the boundary condition at the wall into account ($\delta_{1,N}$ is the Kronecker delta); for (A4) h_0 is replaced by -1, for (A12) by $S_{M,0}$. Equation (A19) gives

$$\left.\begin{aligned} h_1 &= y_1 \\ h_N + u_N\, h_{N-1} &= y_N \,(2 \leqslant N \leqslant s-1) \end{aligned}\right\} \tag{A21}$$

Now, from (A17) all the u_N can be computed and stored in succession, and simultaneously all the y_N from (A20), in descending order. Then from (A21) the h_N can be computed and stored in ascending order.

Using this method, only two sets of auxiliary variables (u_N, y_N) need to be used in the computer, and as they are not required when the h_N have been found, the stores in which one set has been placed can be used for the h_N, successively 'overwriting' the auxiliary variables which are no longer needed. This embodies a slight improvement on the matrix scheme used by Leigh[18] and by Catherall and Mangler[14]; in their matrices the diagonal of 1's appears in $\underline{\underline{L}}$, and another unknown set in the leading diagonal of $\underline{\underline{U}}$, so that this extra unknown set has to be stored as well before calculating h_N. In a small computer such as Mercury, which has only 480 'main variables' in its high speed store, the fewer sets of numbers needed the better; even in its larger counterpart, Atlas, the number of sets of variables used for a given number s of transverse mesh points influences the running cost of the programme.

At the beginning of an iteration the following sets of numbers need to be stored in the high speed store: $\varphi_{M-1,N}$ and $S_{M-1,N}$; $\varphi_{M,N}^{(p-1)}$, $S_{M,N}^{(p-1)}$. We remark that, for the first iteration at a new station, $p = 1$, an obvious choice of first guess is $\varphi_{M,N}^{(0)} = \varphi_{M-1,N}$, $S_{M,N}^{(0)} = S_{M-1,N}$, that is, the values at the previous station. It is convenient to start the iteration with the momentum equation, (A4), even though the vital step – comparison of successive values of $\Delta_M^{(p)}$ with the equation before (48) – is done immediately after this equation has been solved and $\varphi_{M,N}^{(p)}$ found by quadrature. With the h_N representing $G_{M,N}^{(p)}$, the matrix

equations are solved; as $\varphi_{M,N}^{(p-1)}$ are no longer required, the variables u_N are put into their locations and the y_N stored elsewhere, in a fifth set; then in using (A21), the $G_{M,N}^{(p)}$ are put into the y_N locations and the trapezoidal rule

$$\varphi_{M,N} = \int_{\zeta=1}^{\zeta=Na} G_{M,N}\, d\zeta = -[0{\cdot}5\, G_{M,S} + G_{M,S-1} + G_{M,S-2} + \ldots + G_{MN+1} + 0{\cdot}5\, G_{MN}]\, a$$

$$\varphi_{M,S}^{(p)} = 0$$

$$\varphi_{M,N}^{(p)} = \varphi_{M,N+1}^{(p)} - 0{\cdot}5\, a\, (G_{M,N+1}^{(p)} + G_{M,N}^{(p)}) \qquad \text{(A22)}$$

used to calculate $\varphi_{M,N}^{(p)}$ and store them in the u_N locations, which are the old $\varphi_{M,N}^{(p-1)}$ locations. Next the energy equation (A12) is solved; the programming is a little easier because in setting-up the equation (A14) for δ_N^*, the values of $G_{M,N}^{(p)}$ are available immediately (whereas in solving the momentum equation they have to be calculated along with the $G_{M-1,N}$). This time, the matrix variables y_N are put into the $S_{M,N}^{(p-1)}$ locations while the u_N go into the spare set (occupied by $G_{M,N}^{(p)}$); then the h_N (now $S_{M,N}^{(p)}$) are put into the $y_N(S_{M,N}^{(p-1)})$ locations and the cycle is complete.

The necessity for five variable sets restricts Mercury programmes to 96 mesh points including the wall and the outer boundary point, so that the greatest allowable value of s is 95. As it is convenient to use four more variables for storage, this is reduced to 94. It would be possible to add another six points to the mesh by using the 'Page 15' storage with negative indices, but the mystique of 100 mesh points is over-rated here as the significant variable η has a changing range $-\Delta(x) \leqslant \eta \leqslant Y$, so that the mesh values of η will not be 'nice' values in any case. Moreover, the error due to finite a can be significantly reduced by other means (Richardson extrapolation), as explained in Section 4.

The calculation of an initial profile at $x = 0$ (the stagnation point) from which to march is straightforward. At $x = 0$ no x-derivative terms appear in the equations of motion; the partial differential equations therefore become ordinary differential equations in ζ for the profiles of φ and S at $x = 0$, which depend only on ζ. Since q_e is proportional to x near the stagnation point, $E' = x/q_e\, dq_e/dx = 1$ and $H' = 0, G' = F' = 1$. These values are set in the programme, x is of course set to 0, and all reference to the quantities at the last x-station ($\varphi_{M-1,N}$ etc.) is suppressed by setting $\theta = 1$, since these quantities have either x or $(1-\theta)$ as a factor (x occurs in all x-derivative terms, as in (A1), and $(1-\theta)$ in all weighted average terms). (This is why it is convenient to keep θ as a programme variable. θ is set to its averaging value as soon as the initial profiles ($\varphi_{0,N}, S_{0,N}$) have been calculated, ready to march downstream.) As the programme seemed to need much the same number of iterations to converge on the true profiles whatever values of $\varphi_{0,N}$ were fed in as a first guess, and as the $\varphi_{0,N}$ profiles were of different character for negative or positive values of stagnation wall enthalpy $S_B(0)$, the first guess was $\varphi_{0N}^{(0)} = 0$; however, as it was known that $S(0,\eta) \sim e^{-\frac{1}{4}\sigma\eta^2}$ for large η, the first guess for $S_{0,N}^{(0)}$ was $S_B(0) \exp[-\frac{1}{2}\sigma\,(Y+0{\cdot}6479)^2 N^2 a^2]$, the number 0·6479 being the value of $\Delta(0)$ for the incompressible case. This is purely a matter of taste.

APPENDIX B

The Displacement Thickness and Skin Friction

For a compressible boundary layer, the displacement thickness is taken as

$$\delta^* = \int_0^\infty \left(1 - \frac{\rho u}{\rho_e u_e}\right) dy \,. \tag{B1}$$

By (20) and (21)

$$\delta^* = \frac{1}{\rho_e}\left(\frac{\mu_s \rho_s x}{q_e}\right)^{\frac{1}{2}} \int_{-\Delta}^\infty \left(\frac{\rho_e}{\rho} - 1 - \phi_\eta\right) d\eta \tag{B2}$$

$$= \frac{1}{\rho_e}\left(\frac{\mu_s \rho_s x}{q_e}\right)^{\frac{1}{2}} \Delta^* \,. \tag{B3}$$

Making use of (17) and (25), we have

$$\Delta^* = \int_{-\Delta}^\infty \left(\frac{h}{he} - 1\right) d\eta + \Delta \,. \tag{B4}$$

Finally transform to the φ and ζ variables. From (14), (21) and (42)

$$S = \frac{h}{H_s} + \tfrac{1}{2}\frac{q_e^2}{H_s}(\varphi_\zeta + 1)^2 - 1 \,. \tag{B5}$$

Substituting for h from (B5) in (B4) and using (10), also using (38) to change the integrating variable,

$$\Delta^* = \frac{H_s}{h_e} D(x) \int_0^1 \left[S - \frac{q_e^2}{H_s}(\varphi_\zeta + \tfrac{1}{2}\varphi_\zeta^2)\right] d\zeta + \Delta(x) \tag{B6}$$

or, with (32),

$$\Delta^* = \frac{G'}{E'} D \int_0^1 [S - H'(\varphi_\zeta + \tfrac{1}{2}\varphi_\zeta^2)]\, d\zeta + \Delta(x) \,. \tag{B7}$$

The parameter $\Delta(x)$ is therefore related to Δ^* as well as to the boundary conditions at infinity (by (19), (20) and (22)).

In the computational scheme, the value of Δ^*, rather than δ^* given by (B3), is printed out at each step. The ratio δ^*/Δ^* could be calculated if desired, when the variation of viscosity with temperature is

known; for the linear law (29), for example, we find

$$\frac{\delta^*}{\Delta^*} = \frac{1}{\rho_e}\left(\frac{\mu_s \rho_s x}{q_e}\right)^{\frac{1}{2}} = \frac{[H_s/(H_s-\frac{1}{2})]^{\frac{\gamma-2}{2(\gamma-1)}} x^{\frac{1}{2}}}{H_s^{\frac{1}{2}} H'^{\frac{1}{2}} (1-\frac{1}{2}H')^{\frac{1}{\gamma-1}}}. \tag{B8}$$

The integral in (B7) is calculated using Simpson's rule.

The drag per unit length is

$$F_D = \mu_B \left(\frac{\partial u}{\partial y}\right)_B. \tag{B9}$$

On use of (17), (18), (20) and (21)

$$F_D = C_B \left(\frac{\mu_s}{\rho_s}\right)^{\frac{1}{2}} \rho_e \left(\frac{h_e}{H_s}\right) q_e \left(\frac{q_e}{x}\right)^{\frac{1}{2}} (\phi_{\eta\eta})_B. \tag{B10}$$

C_B, the value of C at the wall, can be computed from (29) or (30) and the boundary conditions. After a little algebra to reduce to functions of H_s and H', we find

$$F_D = \frac{C_B}{C_\infty^{\frac{1}{2}}}\left(\frac{H_s}{H_s-\frac{1}{2}}\right)^{\frac{\gamma-2}{2(\gamma-1)}} (H_s H')^{\frac{1}{2}} (1-\tfrac{1}{2}H')^{\frac{\gamma}{\gamma-1}} x^{-\frac{1}{2}} (\phi_{\eta\eta})_B. \tag{B11}$$

Again, only $(\phi_{\eta\eta})_B = D^{-1}(\phi_{\zeta\zeta})_B$ is printed at each step.

We observe that a quantity can in general be found more accurately from first differences than from second differences, because of cut-off of significant figures; thus, ϕ_B'' should be found from the G's rather than the φ's. The programme was therefore written to compute ϕ_B'' while the G's are in the high speed store, after solving the momentum equation.

The formula used in this early attempt was the semi-extrapolation

$$(\phi_{\zeta\zeta})_0 = \frac{1}{12a}[-3\,G_{M,4} + 16\,G_{M,3} - 36\,G_{M,2} + 48\,G_{M,1} - 25\,G_{M,0}] + 0(a^3). \tag{B12}$$

One trouble here is that the $G_{M,N}$ are only correct to $0(a^2)$, so the error in (B12) is really $0(a)$. Later it was realised that a more accurate value could be obtained from the equations at $\zeta = 0$. These equations are not used down to $N = 0$ in the computer scheme as they would contain quantities at the $(M,-1)$ mesh points; however, these fictitious points can be utilised as follows.

The momentum equation at $\zeta = 0$ reduces to:

$$\frac{F'}{D^2}(C\,G_{\zeta\zeta} + C_\zeta\,G_\zeta) + G'(1+S_B) = 0. \tag{B13}$$

If the linear law is being used, this gives further:

$$G_{\zeta\zeta} + \frac{D^2\,G'}{F'}(1+S_B) = 0. \tag{B14}$$

The central difference formulae

$$\left.\begin{aligned} G_{\zeta\zeta} &= \frac{G_{M,1}-2\,G_{M,0}+G_{M,-1}}{a^2} \\ \phi_{\zeta\zeta} &= G_\zeta = \frac{G_{M,1}-G_{M,-1}}{2a} \end{aligned}\right\} + 0(a^2) \tag{B15}$$

are now invoked; eliminating $G_{\zeta\zeta}$ and $G_{M,-1}$ from (B14) and (B15),

$$\phi_{\zeta\zeta} = \frac{1}{2a}\left[2\,G_{M,1}-2\,G_{M,0}+a^2\,D^2\,G'\,(1+S_B)/F'\right]. \tag{B16}$$

On the other hand, if Sutherland's law applies, (B13) and (B14) are not sufficient as the factor C_ζ brings in the value $C_{M,-1}$. We now need the energy equation and the values of C and C_ζ calculated from (30) at $\zeta = 0$. These are:

$$C_\zeta\,S_\zeta + C\,S_{\zeta\zeta} = H'\,(1-\sigma)\,G_\zeta^2 \tag{B17}$$

$$C_B = \frac{(S_B+1)^{\frac{1}{2}}\,B'}{S_B+B'} \tag{B18}$$

$$C_\zeta = C_B\,\frac{S_\zeta(B'-S_B-2)}{2(S_B+B')\,(S_B+1)}. \tag{B19}$$

We may eliminate C_ζ from the momentum and energy equations by (B19):

$$G_{\zeta\zeta}+\frac{B'-S_B-2}{2(S_B+B')\,(S_B+1)}\,S_\zeta\,G_\zeta+\frac{D^2G'}{C_BF'}\,(1+S_B) = 0 \tag{B20}$$

$$S_{\zeta\zeta}+\frac{B'-S_B-2}{2(S_B+B')\,(S_B+1)}\,S_\zeta^2 = \frac{H'(1-\sigma)}{C_B}\,G_\zeta^2 \tag{B21}$$

Write, in this context only,

$$\left.\begin{aligned} g &= \tfrac{1}{8}\,\frac{B'-S_B-2}{(S_B+B')\,(S_B+1)} \\ h &= \frac{a^2\,D^2\,G'}{C_BF'}\,(1+S_B) \\ v &= g\,.\,\frac{H'(1-\sigma)}{4C_B} \end{aligned}\right\} \tag{B22}$$

Similar equations to (B15) can be written down for S_ζ, $S_{\zeta\zeta}$. Eliminating C_B, $G_{M,-1}$ and $S_{M,-1}$ from (B18), (B20), (B21) with (B15), we obtain

$$U = 2a\,\phi_{\zeta\zeta} \tag{B23}$$

where

$$2g(S_{M,1}-S_{M,0})\,U^2+U(2G_{M,1}-2G_{M,0}+h-U)-(2G_{M,1}-2G_{M,0}+h-U)^2-vU^4=0 \qquad \text{(B24)}$$

(B24) is a quartic in U, and an iterative solution with a first approximation from (B12) is the best technique. The Newtonian method is very easily programmed.

Preliminary tests of the new formula indicate some improvement, reduction in oscillation being quite marked, but no results can be given for comparison; (B12) was used in all the runs reported in Section 5.

(B12) is used by itself if Sutherland's law holds and $S_B = -1$ ($S_B < -0{\cdot}99$ in programme).

The heat transfer can also be found from these equations. For the linear law, the energy equation is:

$$S_{\zeta\zeta} = H'(1-\sigma)\,G_\zeta^2 .$$

Writing

$$S_\zeta = \frac{S_{M,1}-S_{M,-1}}{2a} = \frac{W}{a} \qquad \text{(B25)}$$

we then have, after a little algebra,

$$W = S_{M,1}-S_{M,0}-\tfrac{1}{8}H'(1-\sigma)U^2 . \qquad \text{(B26)}$$

On the other hand, for the Sutherland law, we use the transformed momentum equation (B20). Substituting for $G_{\zeta\zeta}$, S_ζ and G_ζ, and using (B22), we find

$$W = \frac{2\,G_{M,1}-2\,G_{M,0}-U+h}{2gU} . \qquad \text{(B27)}$$

This equation is ill-conditioned when $U = 0$, but the programme stops before this point is reached. (B26) or (B27) will give S_ζ, and hence $S_\eta = \dfrac{1}{D}S_\zeta$, when U is known from (B16) or (B24).

APPENDIX C

Computational Details

For the convenience of possible future users, Table 6 lists the contents of the stores in Mercury Autocode. It will be noticed that several of the stores (A, B, B', D, E', F', G', H', X, Y) have been chosen to match the quantities mentioned in the text. It will also be noted that most of the 'special' variable space has been used; only C' remains unoccupied. This seems to be the bare minimum required.

The programme is divided into five chapters; Chapter 1 reads in data and sets the machine to calculate profiles at the stagnation point if this has not been done; Chapter 2 holds the iteration scheme; Chapter 3 sets the outer-edge (inviscid solution) variables E', F', G' and H' at both mean and end stations, and the enthalpy boundary condition, and performs any other calculation that may be required; in Chapter 4 the solution variables for the smaller step length are read into the drum (backing store), along with Δ, Δ^* and ϕ''_B, while the solution for the larger step length is calculated, and Richardson extrapolation is performed on the two sets; in Chapter 0 the values of the three parameters are printed at each downstream step, with additional data if desired, x is increased to its new value and θ is reset in accordance with (83) every time x passes through a value $0{\cdot}1L$. In any programme, therefore, only Chapter 3 will need alteration; it should be remembered that X has been set to its mean station value, x_θ say, on entry into the chapter, so that if, say, the wall enthalpy S_B is a function of x, it must be calculated at the end station using $Z = x_\theta + b(1-\theta)$, and its value put into the store H_0. So should any other functions required (for instance, edge velocity).

The values of the four parameters E', F', G' H' and G'/E' at the end station are needed in Chapter 4 to calculate the displacement thickness and skin friction (*see* Appendix B). These values are held in main variables V_0, V_1, V_2, V_3, E respectively. With 94 steps, there is room in the Mercury high speed store for these.

The initial data tape must be prepared as follows:

0 if data tape required; 1 otherwise

Mach number ($\neq 0$)

Convergence parameter (10^{-5} usual)

Outer limit Y

Number of transverse steps s (must be even and $\leqslant 200$)

Downstream steplength $b(\neq 0$; should be divisible into $0{\cdot}1$)

Prandtl number σ

The integer L; machine will stop at $x = 0{\cdot}1L$ and read in a new case

B' (set to value given by (31) if Sutherland law used; set to -1 if linear law used)

The boundary value $S_B(0)$

Weight parameter θ.

The first number (0 or 1) directs the machine to calculate a stagnation profile. In data tapes output downstream this number is replaced by 2; then the first eight numbers printed are as above, and are followed by necessary station details.

The values of Y (which is actually called ETA_0 here), s and b and the convergence parameter are printed out on a line at the top of the page before any calculations are performed, for example:

$$ETA_0 = 6 \quad S = 94 \quad B = 0{\cdot}010 \quad \text{ACCURACY } 1{\cdot}0,-5.$$

This is followed on the next line by actual problem details: σ, the viscosity law, value of $S_g \equiv H_0$, and

Mach number, for instance.

SIGMA = 0·72 LINEAR LAW $S(B) = -1{\cdot}00$ $M = 0{\cdot}5$

This may help in filing results.

The value B' is used to determine which law is used. If it is a number less than 0, the linear law is used; it is chosen in this way to avoid one possible division by zero. By (31) or (92), for the Sutherland law $B' > 1$, and so no confusion can arise between the two laws.

When testing to find optimum values of θ, there is little point in having separate tape outputs for each trial value, and each output currently costs 10/–; consequently, when starting from $x = 0$, the first number should be set to 0 only if a tape output is required at the end of the run, and to 1 if no output is required, as in the trial runs. If this number is set to 0, so that there is output, the new first number on the tape will now be 2; should this be read in again, unchanged, a data tape will again be provided at the end of the new run, but if it should happen that no further data output is required, this first number (2) should be altered to 3. This can easily be done by hand on the tape, punching two extra holes.

For the trial runs a value of L should be set to that $x = 0{\cdot}1L$ embraces 20 downstream steps or so, say $L = 2$. The outputs can then be inspected and tested for oscillation, for the final run without halt, L can be set to -1.

The programme will also stop, and produce tape output or not according to the above, when the last value calculated for ϕ''_B falls below 0·1, that is, when separation is near. This criterion can be adjusted if desired, at label 5 for Chapter 0.

Finally, at Label (2) of Chapter 3 the programmer must write his own routine for calculating E' and H' as functions of the variable $Z(\equiv x)$ and storing them in V_0 and V_3. The programme then calculates F', G' (V_1, V_2) and E. The Mach number is stored in U' for evaluating H_s by (10) and (11), and hence H'.

LIST OF SYMBOLS

a_e, a_s	Sound velocities
a	Transverse step length
b	Downstream step length
B'	$1+S_u/H_s$
c, C^*	Cohen and Reshotko constants
C	Viscosity factor
D	$Y+\Delta(x)$
E'	$\frac{x}{q_e}\frac{dq_e}{dx}$
f	Cohen and Reshotko transformed stream function
F'	$h_e \rho_e / H_s \rho_s$
F_D	Skin-friction drag per unit length
G	$\partial\phi/\partial\eta$
G'	$\frac{H_s}{h_e}E'$
h	Scaled enthalpy
H_s	Free stream stagnation enthalpy (scaled)
H	h_e/H_s
H'	q_e^2/H_s
J	Catherall and Mangler variable
l	Characteristic length scale
L	Integer denoting downstream stations $x = 0{\cdot}1L$
m	Cohen and Reshotko similarity parameter
M	Mach number
p	Scaled pressure
q_e	Velocity (u) at outer edge of boundary layer
R	Reynolds number $\rho_\infty l U_\infty/\mu_\infty$
s	Number of transverse steps
S	Enthalpy function
S_u	Sutherland constant
S_0	$S(0,\eta)$; stagnation point profile
T	Temperature (°K)
u	Dimensionless velocity in x direction
U_∞	Free stream velocity (unscaled)

v	$R^{\frac{1}{2}} v^*$
v^*	Dimensionless velocity in y direction
x	Dimensionless arc distance downstream from stagnation point
X	Cohen and Reshotko downstream co-ordinate
y	$R^{\frac{1}{2}} y^*$
y^*	Dimensionless distance measured normal to body surface
Y	Value of η representing outer edge of boundary layer
β	Cohen and Reshotko pressure gradient parameter
γ	Ratio of specific heats
δ^*	Displacement thickness
$\Delta(x)$	Transform variable
Δ_{CM}	$\Delta(x)$ calculated from Catherall and Mangler series solution
Δ_{CR}	Cohen and Reshotko check parameter $\Delta(x)\dfrac{\eta^*(x)}{\eta(x)}$
ζ	Transformed η for computer scheme
η	Transformed transverse co-ordinate
η^*	Transformed Cohen and Reshotko transverse co-ordinate
θ	Weight parameter
θ_0	Value of θ for $0 < x \leqslant 0{\cdot}1$
μ	Scaled viscosity
ξ	Catherall and Mangler downstream co-ordinate
ρ	Scaled density
σ	Prandtl number
ϕ	Transformed stream function
ϕ_0	$\phi(0, \eta)$; stagnation profile
ϕ''_B	Convenient notation for skin-friction parameter $\left(\dfrac{\partial^2 \phi}{\partial \eta^2}\right)_B$
φ	Transformed ϕ for computer scheme
ψ	Stream function
Ψ	Cohen and Reshotko stream function
ω	Viscosity-temperature index
	Suffixes
∞	Free-stream value
s	Free-stream stagnation value

LIST OF SYMBOLS—*continued*

e	Value at outer edge of boundary layer
B	Value at body surface
$N, N\pm1$, etc	Value at (Nth, etc.) transverse mesh point
M, N	Value at M-th downstream station and N-th mesh point
	Superscripts
(p)	Value of unknown field variable found in p-th iteration cycle
Overbar	Weighted average value for neighbouring x-stations

REFERENCES

No.	*Author(s)*	*Title, etc.*
1	L. Prandtl	Über Flüssigskeitsbewegung bei sehr kleiner Reibung. *Proceedings of the 3rd Mathematical Congress*, Heidelberg (1904). English version: Tech. Memor. nat. adv. Comm. Aero., Wash. No. 452.
2	T. von. Kármán	The problem of resistance in compressible fluids. *Convegno di Scienze Fisiche Matematiche e Naturali.* (5th Volta Congress) pp. 222–277 (1935).
3	D. R. Chapman and M. W. Rubesin ..	Temperature and velocity profiles in the compressible laminar boundary layer with arbitrary distribution of surface temperature. *J. Aero. Sci.* 16, pp. 547–565 (1949).
4	L. Howarth	Concerning the effect of compressibility on laminar boundary layers and their separation. *Proc. R. Soc.* London. A 194, p. 16 (1948).
5	K. Stewartson	Correlated incompressible and compressible boundary layers. *Proc. R. Soc.* London. A 200, p. 84 (1949).
6	C. B. Cohen and E. Reshotko	Similar solutions for the compressible laminar boundary layer with heat transfer and pressure gradient. NACA Rep. 1293, (1956).
7	J. F. Gross and C. F. Dewey	Similar solutions of the laminar boundary layer equations with variable fluid properties. Memorandum RM–3792–PR, California (1963).
8	N. Curle	*The laminar boundary layer equations.* Oxford U.P. (1962).
9	A. D. Young	The effects of small change of Prandtl number and the viscosity-temperature index on skin friction. *Aeronaut. Q*, XV (4) pp. 392–406 (1964).

REFERENCES—*continued*

No.	*Author(s)*	*Title, etc.*
10	F. W. Matting	General solution of the laminar compressible boundary layer in the stagnation region of blunt bodies in axisymmetric flow. NASA TN D–2234, (1964).
11	K. W. Mangler	Zusammenhang zwischen ebenen und rotations-symmetrischen Grenzschichten in kompressiblen Flüssigkeiten. *Z. angew. Math. Mech.* 28, p. 97 (1948).
12	A. M. O. Smith and D. W. Clutter ..	Solution of Prandtl's boundary layer equations. Douglas Aircraft Engineering Paper 1530, California (1963).
13	I. Flügge-Lotz and F. G. Blottner	Computation of the compressible laminar boundary layer flow including displacement-thickness iteration using finite difference methods. Stanford University Division of Engineering Mechanics, Tech. Report 131 (1962).
14	D. Catherall and K. W. Mangler	An indirect method for the solution of the Navier-Stokes equations for laminar incompressible flow at large Reynolds numbers. R.A.E. Report No. Aero 2683 (1963). A.R.C. 25 599.
15	K. Stewartson	Behaviour of a laminar compressible boundary layer near a point of zero skin friction. *J. Fluid Mech.* 12, p. 117–128 (1962).
16	S. Goldstein	On backward boundary layers and flow in converging passages. *J. Fluid Mech.* 21, p. 33–45 (1965).
17	J. Crank and P. Nicolson ..	A practical method for numerical evaluation of solutions of partial differential equations of the heat-conduction type. *Proc. Camb. Phil. Soc.* 43, p. 50 (1947).
18	D. C. F. Leigh	The laminar boundary layer equations; a method of solution by means of an automatic computer. *Proc. Camb. Phil. Soc.* 51, p. 320 (1955).
19	C. B. Cohen and E. Reshotko	The compressible laminar boundary layer with heat transfer and arbitrary pressure gradient. NACA Rep. 1294, Washington (1956).
20	D. Catherall	Private communication (1965).
21	R. J. Monaghan	Formulae and approximations for aerodynamic heating rates in high speed flight. A.R.C. C.P. 360.
22	R. D. Richtmyer	*Difference methods for initial value problems.* Interscience, New York (1957).
23	R. M. Terrill	Laminar boundary-layer flow near separation with and without suction. *Phil. Trans. Roy. Soc.* A 253, p. 55 (1960).

TABLE 1

Comparison with Cohen and Reshotko Similar Solution

η^*	U (Current programme)	U (Cohen and Reshotko)	S (Current programme)	S (Cohen and Reshotko)
0	0	0	1·0000	1·0000
0·2	0·3077	0·3084	0·8770	0·8770
0·4	0·5434	0·5439	0·7548	0·7549
0·6	0·7160	0·7165	0·6356	0·6357
0·8	0·8366	0·8370	0·5221	0·5223
1·0	0·9164	0·9167	0·4174	0·4176
1·2	0·9657	0·9659	0·3241	0·3243
1·4	0·9935	0·9936	0·2441	0·2444
1·6	1·0072	1·0073	0·1780	0·1783
1·8	1·0121	1·0122	0·1256	0·1259
2·0	1·0124	1·0123	0·0857	0·0860
2·2	1·0104	1·0104	0·0564	0·0568
2·4	1·0079	1·0078	0·0359	0·0363
2·6	1·0055	1·0053	0·0220	0·0224
2·8	1·0036	1·0034	0·0131	0·0134
3·0	1·0022	1·0020	0·0075	0·0078
3·2	1·0013	1·0010	0·0041	0·0045
3·4	1·0007	1·0003	0·0022	0·0026
3·6	1·0004	0·9999	0·0011	0·0015
3·8	1·0002	Not given	0·0005	Not given
4·0	1·0001	Not given	0·0003	Not given

TABLE 2

Effect of θ on Cohen and Reshotko Parameter Δ_{CR}

x	Δ_{CR} $\theta = 0{\cdot}5$	Δ_{CR} $\theta = 0{\cdot}75$
0·00	0·425000	0·425000
0·01	0·424991	0·425000
0·02	0·425007	0·425002
0·03	0·424981	0·425001
0·04	0·425020	0·425002
0·05	0·424976	0·425002
0·06	0·425021	0·425003
0·07	0·424973	0·425003
0·08	0·425024	0·425003
0·09	0·424971	0·425004
0·10	0·425025	0·425004
0·11	0·424969	0·425004
0·12	0·425026	0·425005
0·13	0·424968	0·425005
0·14	0·425025	0·425005
0·15	0·424968	0·425005
0·16	0·415024	0·425005
0·17	0·414987	0·425005
0·18	0·425029	0·425006
0·19	0·424975	0·425006
0·20	0·425023	0·425005
0·21	0·424962	0·425005
0·22	0·425025	0·425005
0·23	0·424951	0·425005
0·24	0·425030	0·425005
0·25	0·424939	0·425005
0·26	0·425038	0·425005
0·27	0·424928	0·425004
0·28	0·425051	0·425004
0·29	0·424925	0·425004
0·30	0·425074	0·425003

TABLE 3

Variation of Displacement Thickness with Wall Enthalpy

S_B	Δ^* (Cohen and Reshotko)	Δ^* (current programme)
−1	−0·170	−0·157738
−0·8	0·012	0·011251
−0·4	0·345	0·336312
0	0·648	0·647901
1·0	1·386	1·384477
2·0		2·077437

TABLE 4

Stagnation Values Comparison. $\sigma = 0{\cdot}7$

		Linear law $S_B = -0{\cdot}4$	Linear law $S_B = -0{\cdot}5$	Sutherland law $S_B = -0{\cdot}3$	Sutherland law $S_B = -0{\cdot}4$
Δ	Matrix	0·785473	0·824124	0·769625	0·814095
	Runge-Kutta	0·785187	0·823987	0·769012	0·813597
Δ^*	Matrix	0·293197	0·202367	0·395122	0·305946
	Runge-Kutta	0·292932	0·202178	0·394591	0·305562
ϕ''_B	Matrix	0·99783	0·93588	1·01625	0·94769
	Runge-Kutta	0·99770	0·93622	1·01671	0·94749

TABLE 5

Viscosity Laws Compared at Stagnation Point. $\sigma = 0{\cdot}7$

	$S_B = -0{\cdot}5$			$S_B = 1{\cdot}0$		
	Linear law	Sutherland law	Difference %	Linear law	Sutherland law	Difference %
Δ	0·824124	0·860360	4·4	0·381559	0·344717	9·7
Δ^*	0·202367	0·214067	5·8	1·487935	1·375699	7·5
ϕ''_B	0·93588	0·88070	5·9	1·76553	1·97564	11·9

TABLE 6

Contents of Computer Stores

Special variables

	Plain	Dashed
A	a (step length)	$G^{(p)}_{M,N+1}$
B	b (step length)	$1+S_w/H_s$
C	σ	
D	$D^{(p)}_M$	D_{M-1}
E	H_s/h_e	$\frac{x}{q_e}\frac{dq_e}{dx}$
F	Slave	$\frac{\rho_e h_e}{\rho_s H_s}$
G	$\frac{\Lambda}{2a}$	$E'\frac{H_s}{h_e}$
H	C_N£′	q_e^2/H_s
U	$(\phi''_B)_M/D_M$	Mach number
V	$1+\bar{G}_N$ (weighted velocity)	Convergence parameter
W	oscillation test variable	$\varphi^{(p)}_{M,N+1}$
X	x; x_θ; x_θ/b	θ
Y	Y	$1-\theta$
Z	Slave	Slave
£(π)	$1/D_\theta$	$F'/a^2D_\theta^2$

Indices

	Plain	Dashed
I		
J	Slave	
K	$0{\cdot}1/B$	10 times under relaxation factor
L	$X = 0{\cdot}1L+MB$	Stop when $L = L'$
M	$1 \leqslant M \leqslant K$	
N	Cycles	Cycle counter
O	oscillation counter	
P	Set to 1 when $D^{(p)}_M$ converges	
Q	0 (momentum equation) 1 (energy equation)	
R	S−1	$0{\cdot}5\,S'$
S	$1/A$; R' or S'	Largest No. of steps
T	0 or 2 stagnation point 1 or 3 downstream	

Main variables

E_N	$S_{M-1,N}$	
H_N	$S^{(p-1)}_{M,N}$	$(Q=0)$
	matrix y_N	
	$S^{(p)}_{M,N}$	$(Q=1)$
F_N	$\varphi_{M-1,N}$	
U_N	$\varphi^{(p)}_{M,N}$	$(Q=1)$
	matrix variables u_N	
	$\varphi^{(p+1)}_{M,N}$	$(Q=0)$
G_N	matrix y_N	
	$G^{(p)}_{M,N}$	$(Q=0)$
	matrix u_N	$(Q=1)$

C_N	Weighted Sutherland viscosity factors $\bar{C}_N$
V_0, V_1, V_2 V_3	Values of E', F', G', H' at end stations.

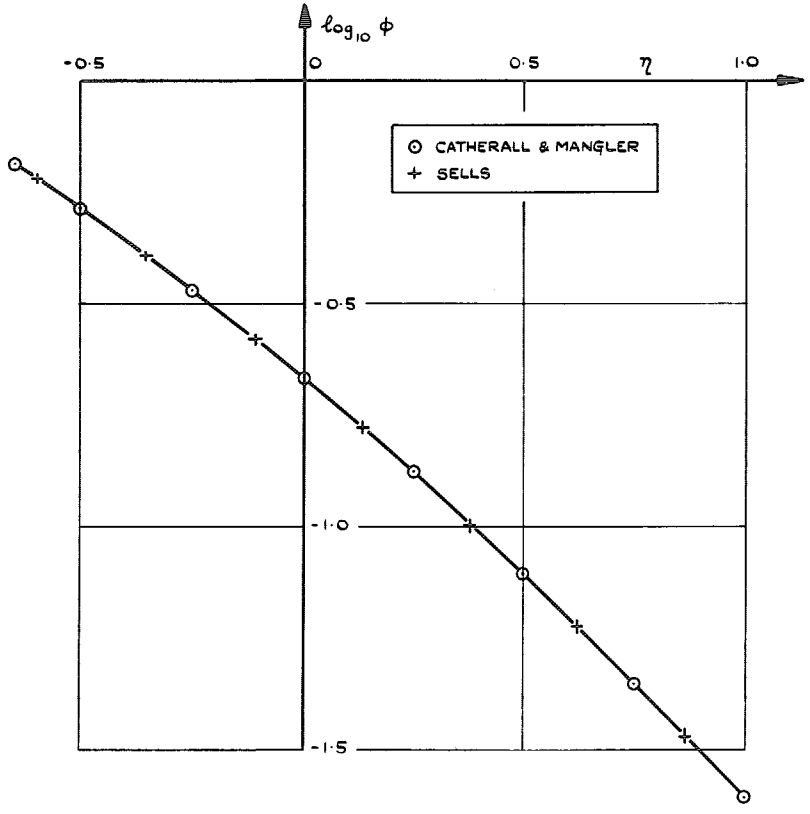

FIG. 1. Incompressible stagnation point profile.

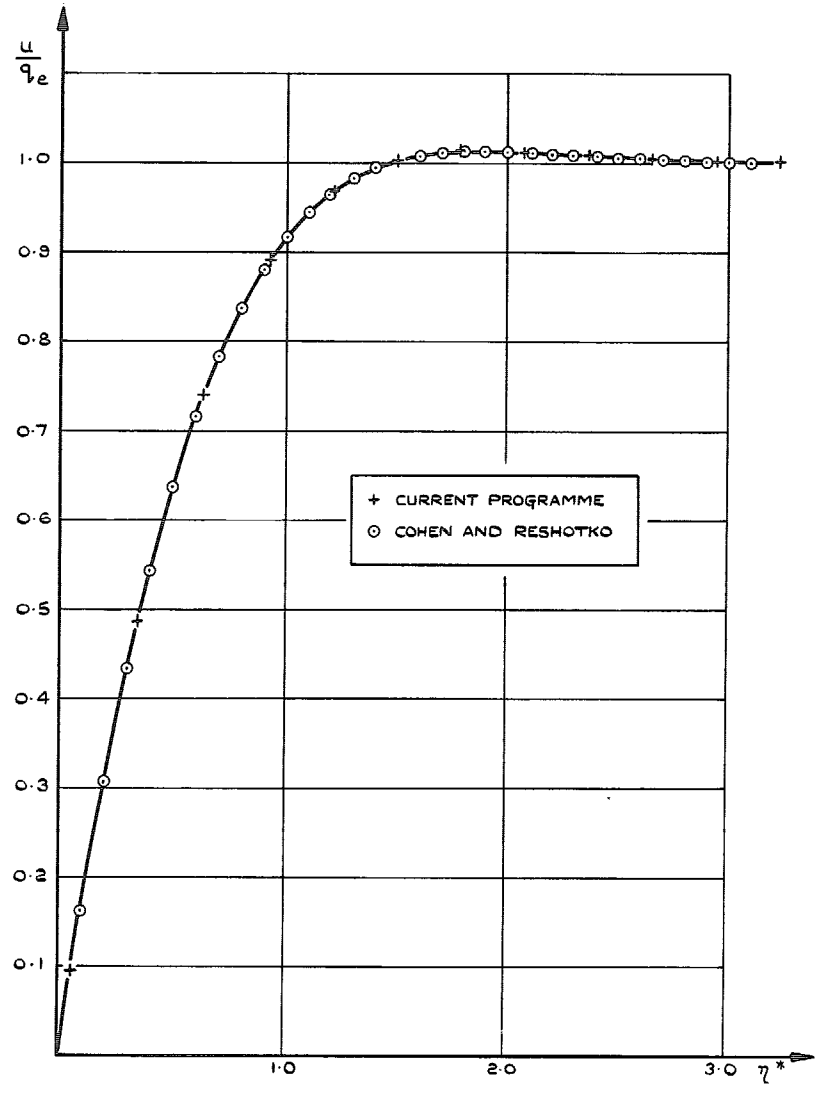

FIG. 2. Cohen and Reshotko similar solution ($S_B = 1{\cdot}0$).

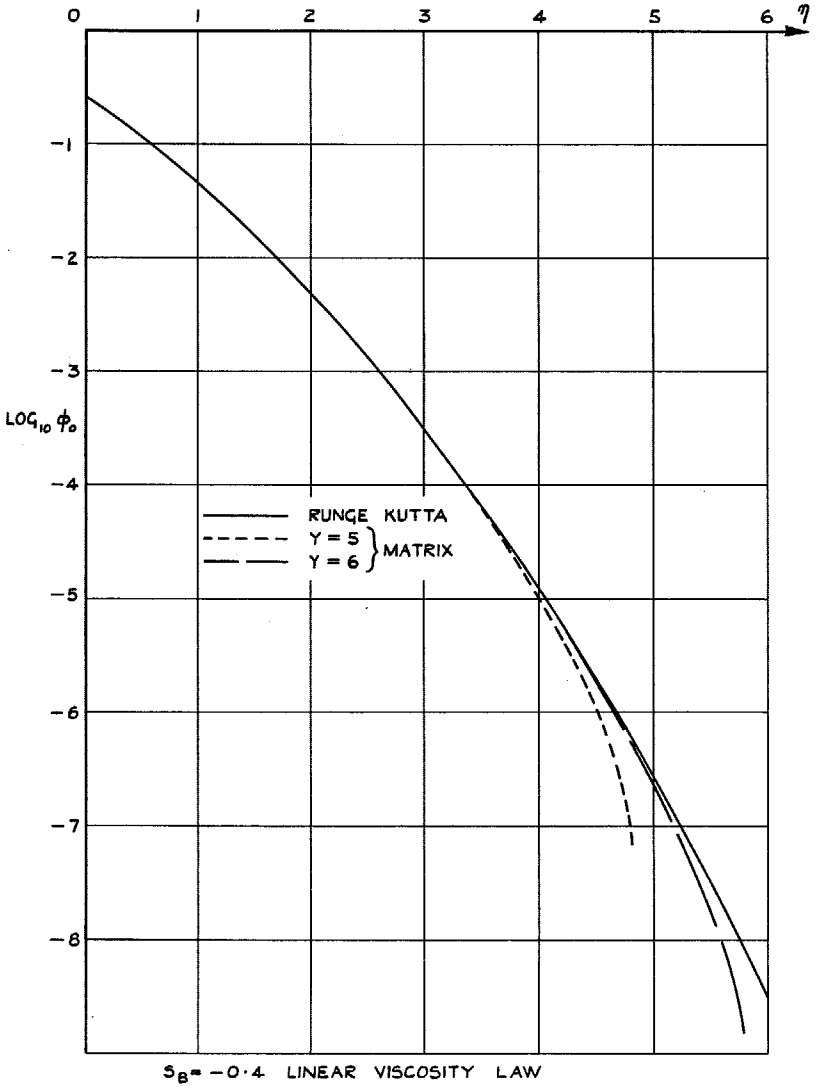

FIG. 3. Comparison of methods of calculating stagnation profiles.

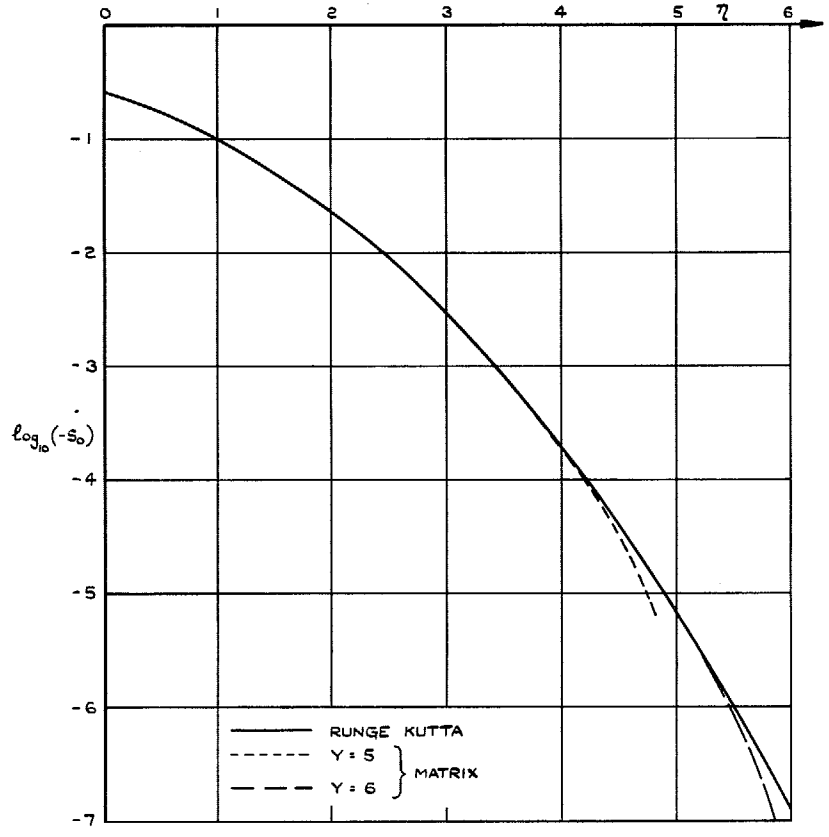

FIG. 4. Comparison of methods for S_0.

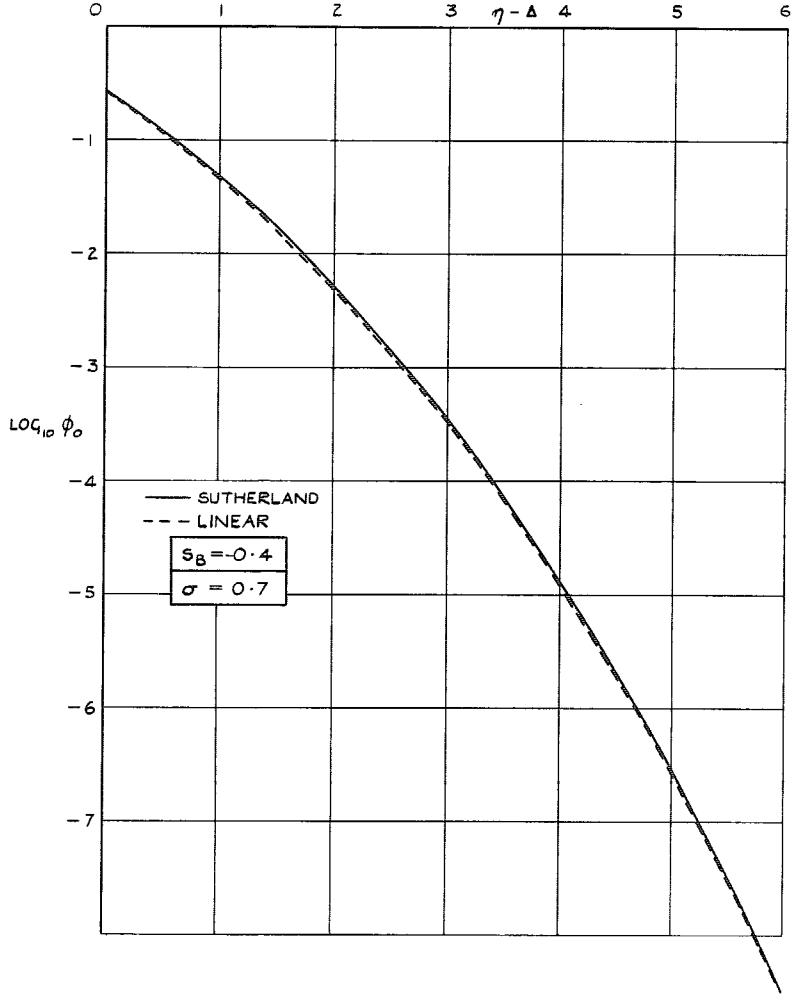

FIG. 5. Comparison of linear and Sutherland stagnation profiles.

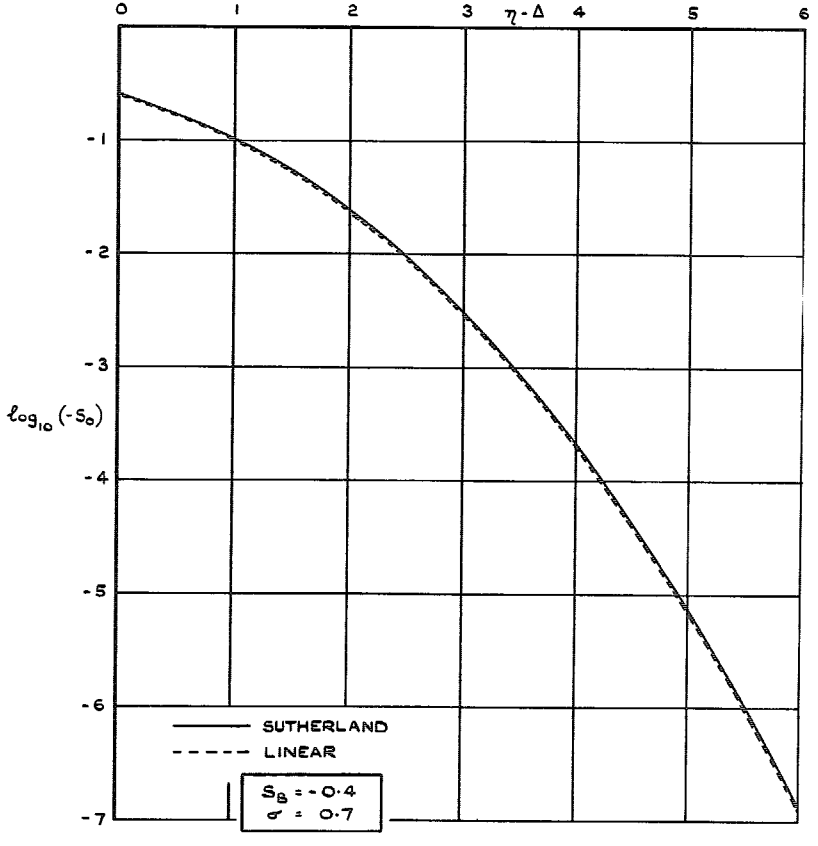

FIG. 6. Comparison of linear and Sutherland stagnation profiles.

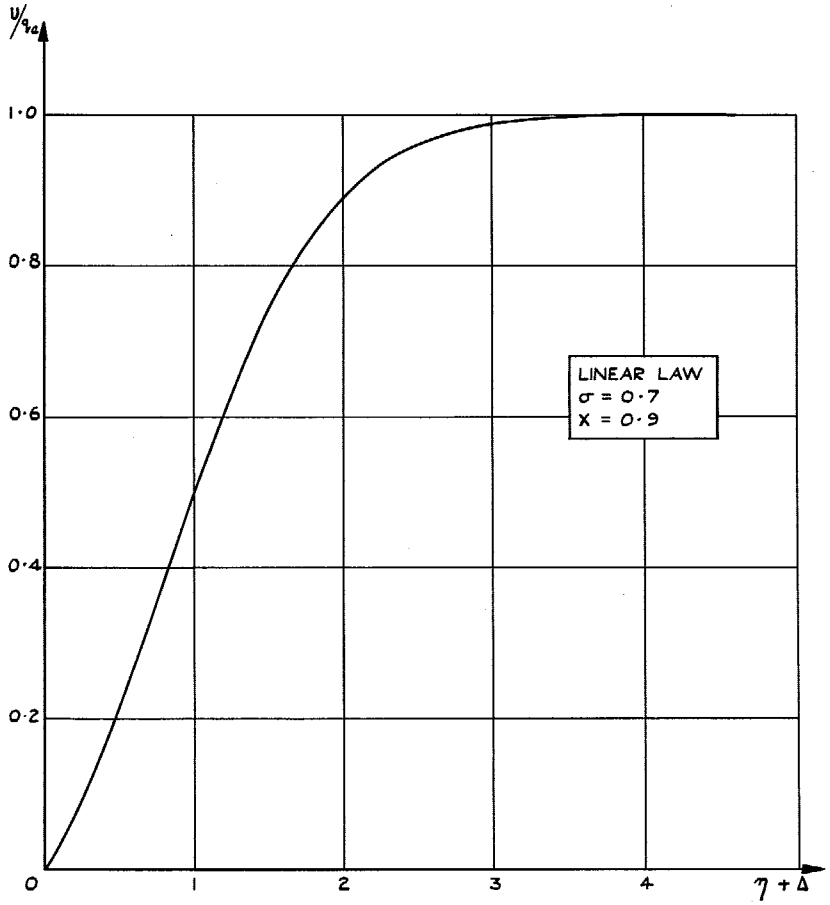

FIG. 7. Velocity profile near separation on cooled cylinder.

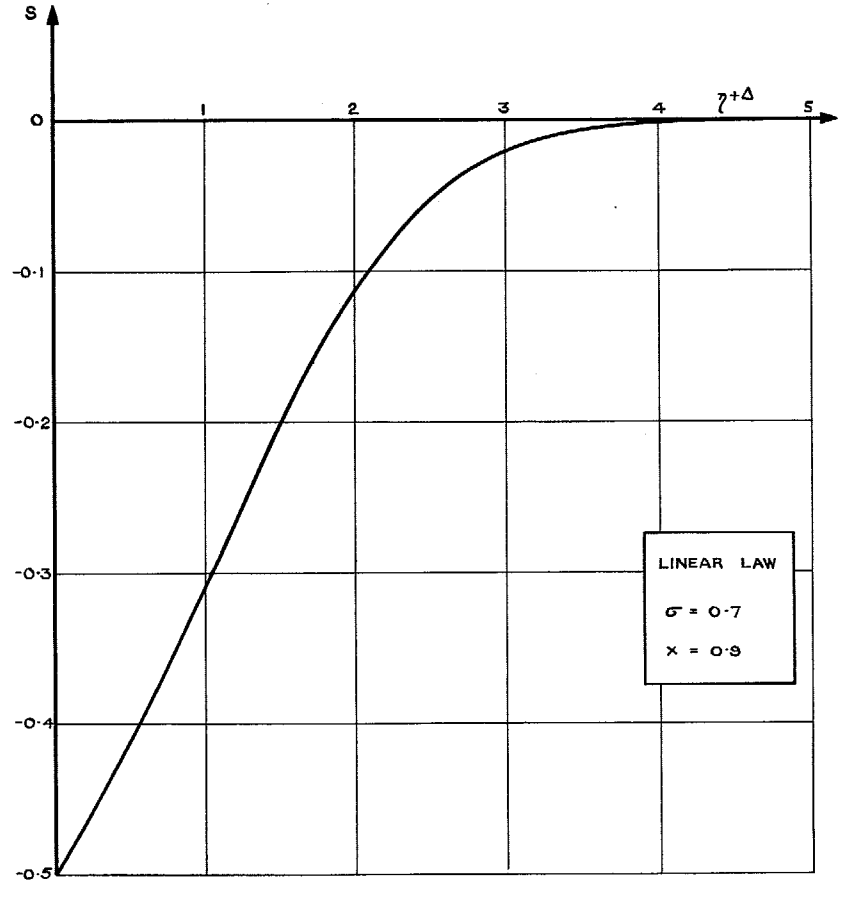

FIG. 8. Enthalpy profile near separation on cooled cylinder.

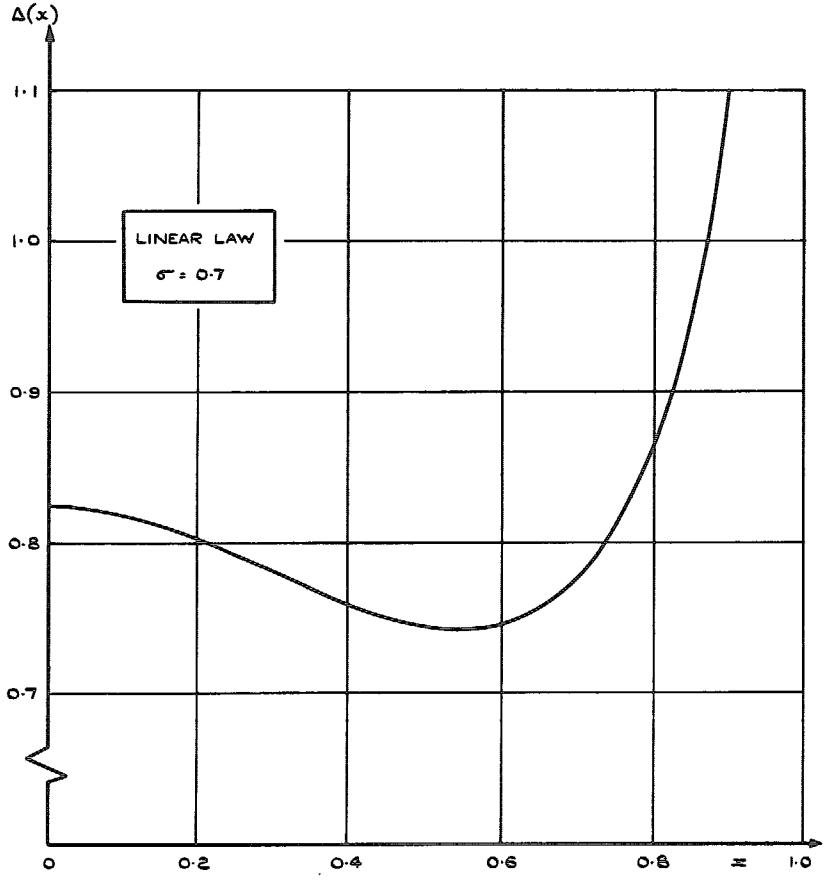

FIG. 9. $\Delta(x)$ for cooled cylinder.

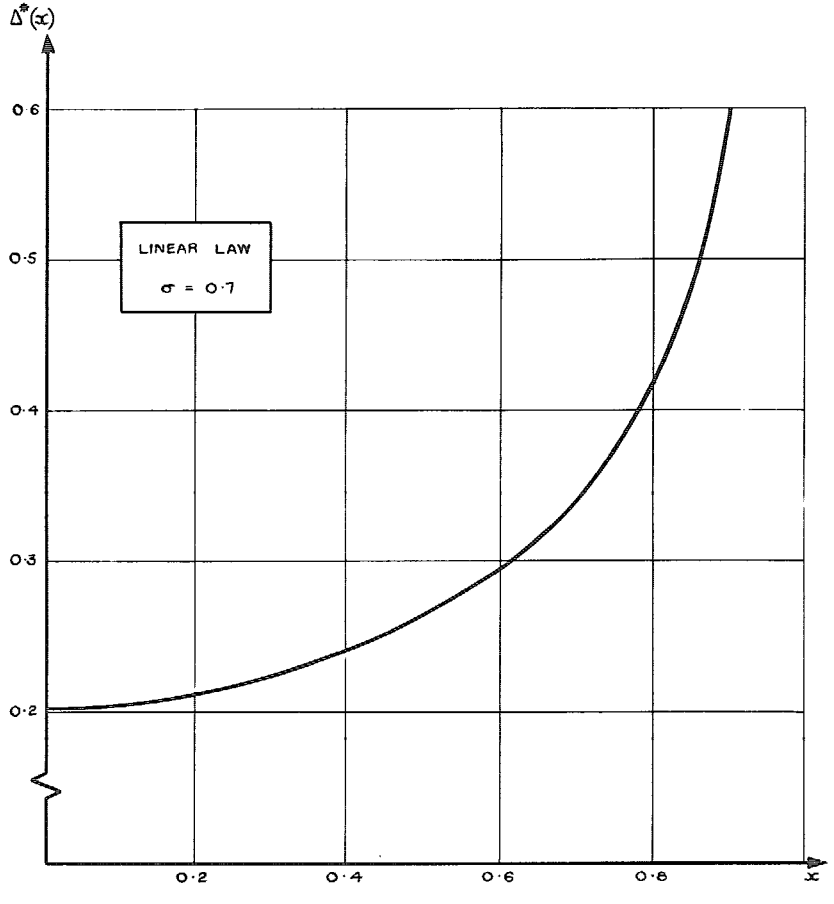

FIG. 10. Displacement thickness for cooled cylinder.

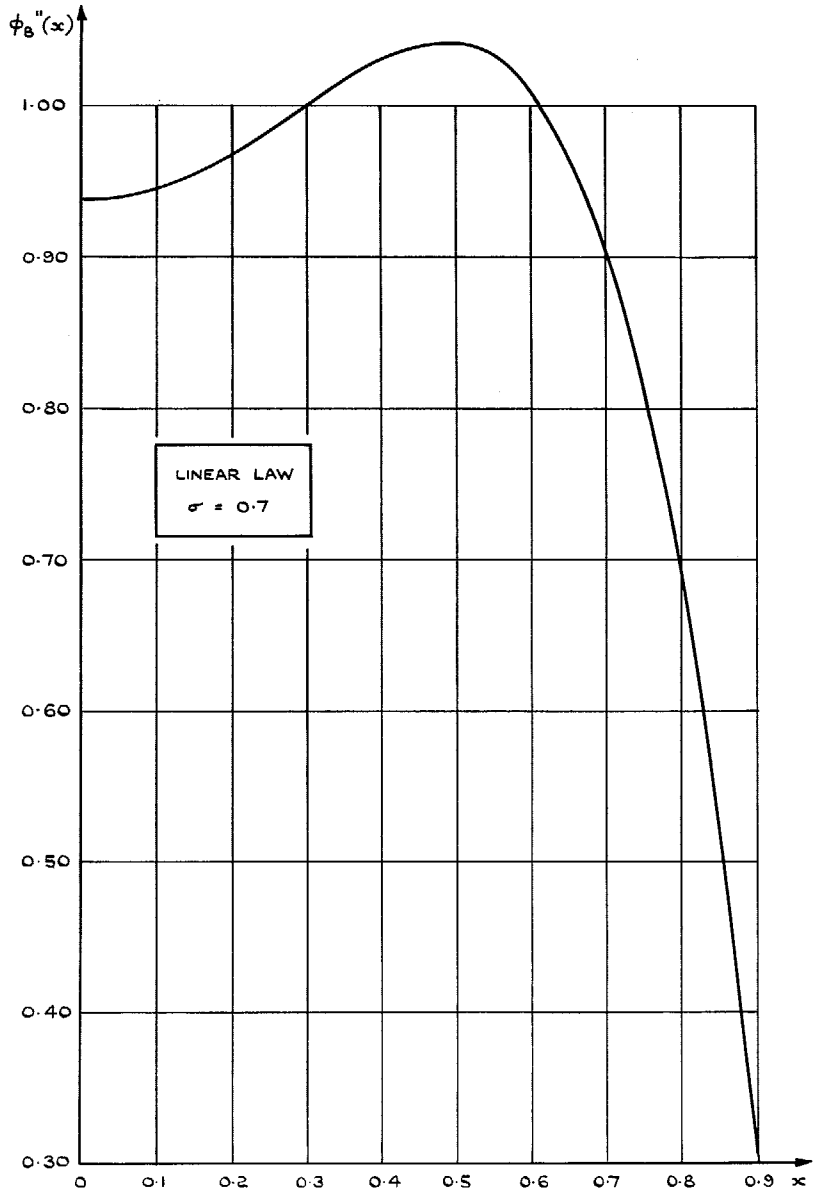

FIG. 11. $\phi_B''(x)$ for cooled cylinder.

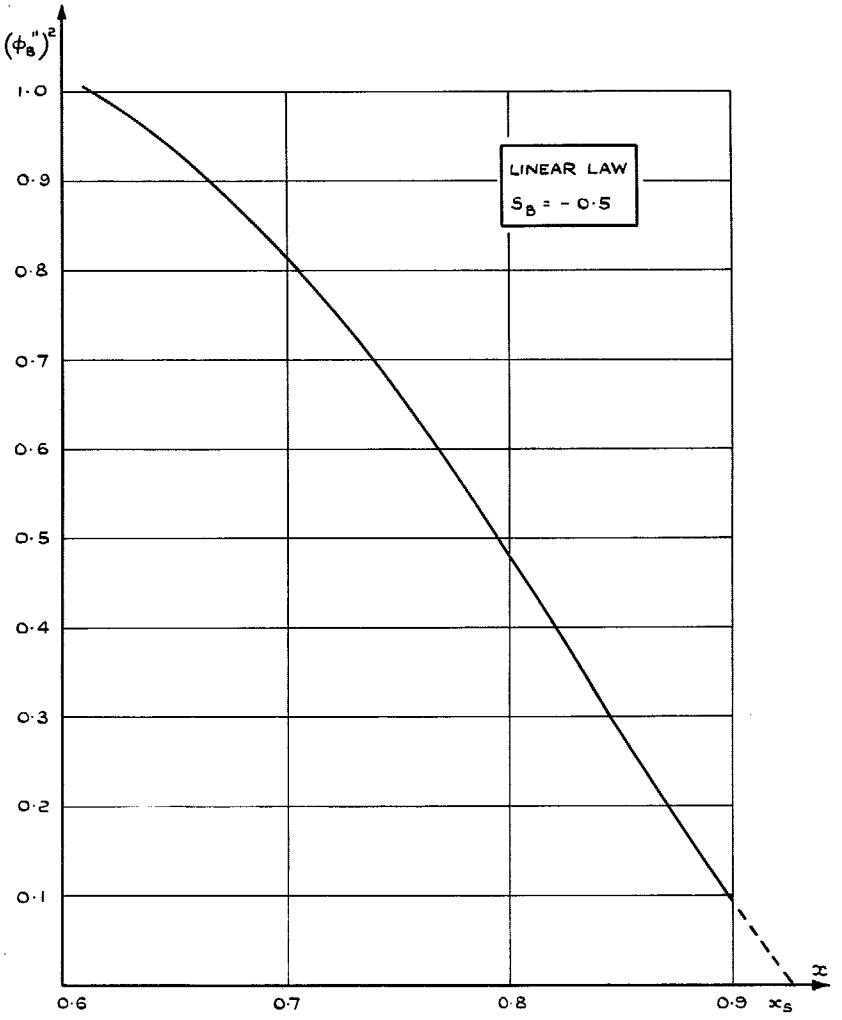

FIG. 12. Behaviour of ϕ_B'' near separation: $\phi_B'' \sim (x_s - x)^{\frac{1}{2}}$.

Printed in Wales for Her Majesty's Stationery Office by Allens Printers (Wales) Limited

Dd.129527 K.5

Published by
HER MAJESTY'S STATIONERY OFFICE

To be purchased from
49 High Holborn, London W.C.1
13a Castle Street, Edinburgh 2
109 St. Mary Street, Cardiff CF1 1JW
Brazennose Street, Manchester 2
80 Chichester Street, Belfast
or through any bookseller